Wet deposition of atmospheric inorganic nitrogen at five remote sites on the Tibetan Plateau

Y. W. Liu[1,3], Xu-Ri[1,2], Y. S. Wang[4], Y. P. Pan[4], and S. L. Piao[1,2,3]

[1]Key Laboratory of Alpine Ecology and Biodiversity, Institute of Tibetan Plateau Research, Chinese Academy of Sciences, Beijing 100101, China

[2]CAS Center for Excellence in Tibetan Plateau Earth Sciences, Beijing 100101, China

[3]Sino-French Institute for Earth System Science, College of Urban and Environmental Sciences, Peking University, Beijing 100871, China

[4]State Key Laboratory of Atmospheric Boundary Layer Physics and Atmospheric Chemistry (LAPC), Institute of Atmospheric Physics, Chinese Academy of Sciences, Beijing 100029, China

Correspondence to: Xu-Ri (xu-ri@itpcas.ac.cn)

Abstract

Since the mid-20th century, nitrogen (N) deposition has shown an increasing trend on the Tibetan Plateau (TP), where alpine ecosystems are sensitive to elevated N deposition. However, the quantitative characterization of N deposition on the TP remains unclear, due in most part to the lack of *in situ* measurement. Using the Tibetan Observation and Research Platform network, we conducted short-term *in situ* measurements of major ions (NO_3^-, Cl^-, SO_4^{2-}, NH_4^+, Na^+, K^+, Ca^{2+} and Mg^{2+}) wet deposition at five remote sites on the TP during 2011-2013. At Southeast Tibet Station, Nam Co Station, Qomolangma Station, Ngari Station, and Muztagh Ata Station, the NH_4^+-N wet deposition was 0.63, 0.68, 0.92, 0.36 and 1.25 kg N ha^{-1} yr^{-1}, respectively; the NO_3^--N wet deposition was 0.28, 0.24, 0.03,

0.08 and 0.30 kg N ha^{-1} yr^{-1}, respectively; and the inorganic N deposition was 0.91, 0.92, 0.94, 0.44 and 1.55 kg N ha^{-1} yr^{-1}, respectively. The inorganic N wet deposition mainly occurred as the form of NH_4^+-N during the summer at all stations. Results of enrichment factor analysis and principal component analysis demonstrated that both NH_4^+-N and NO_3^--N wet deposition on the TP were mainly influenced by anthropogenic activities. Backward trajectory analysis showed that the inorganic N deposition at Muztagh Ata Station was mainly transported from Central Asia and Middle East through westerlies. At Southeast Tibet Station, Nam Co Station, Qomolangma Station and Ngari Station, the inorganic N deposition was mainly contributed by anthropogenic sources in South Asia, and was mainly transported by Indian monsoon. Combining site-scale *in situ* measurements of inorganic N wet deposition in this and previous studies, the average wet deposition of atmospheric NH_4^+-N, NO_3^--N, and inorganic N on the TP was estimated to be 1.09, 0.57 and 1.66 kg N ha^{-1} yr^{-1}, respectively. The average NH_4^+-N:NO_3^--N ratio in precipitation on the TP was 2:1. Compared to the present study, previous regional-scale estimation of inorganic N wet deposition for the entire TP, either through atmospheric chemistry transport model simulations or interpolations based on limited field observations, has been highly overestimated. To clarify the total N deposition on the TP more clearly, it is essential to conduct long-term monitoring of both wet and dry deposition of atmospheric N in various climate zones on the TP in the future.

1 Introduction

The global nitrogen (N) cycle has been disturbed by elevated reactive N emissions from anthropogenic activities since the mid-19th century (Canfield et al., 2010; Galloway et al., 2008; Gruber and Galloway, 2008). Accumulated reactive N in the environment has led to a series of effects on climate change and ecosystems, e.g. air pollution, stratospheric ozone depletion, the potential alteration of global

temperature, drinking water contamination, freshwater eutrophication, biodiversity loss, grassland seed bank depletion, and dead zones in coastal ecosystems (Basto et al., 2015; Erisman et al., 2011; Erisman et al., 2013; Lan et al., 2015; Pinder et al., 2012; Shi et al., 2015; Zaehle et al., 2010). To examine the actual amount of N inputted into ecosystems, several monitoring networks have been established at national or continent scales, e.g. the National Atmospheric Deposition Program National Trends Network (NADP/NTN, United States) (Lehmann et al., 2005), the Canadian Air and Precipitation Monitoring Network (CAPMoN, Canada) (Zbieranowski and Aherne, 2011), the European Monitoring and Evaluation Programme (EMEP, Europe) (Fagerli and Aas, 2008), the Austrian Precipitation Sampling Network (Austria) (Puxbaum et al., 2002), and the Japanese Acid Deposition Survey (JADS, Japan) (Morino et al., 2011).

Besides Europe and North America, East Asia has become another high N deposition region, due to rapid economic growth in recent decades (Dentener et al., 2006). Across China, inorganic N wet deposition has increased since the mid-20th century, albeit with inconsistent estimations of the change: 8 kg N ha^{-1} yr^{-1} (from 13.2 kg N ha^{-1} yr^{-1} in the 1980s to 21.1 kg N ha^{-1} yr^{-1} in the 2000s) (X. J. Liu et al., 2013); 2.8 kg N ha^{-1} yr^{-1} (from 11.11 kg N ha^{-1} yr^{-1} in the 1980s to 13.87 kg N ha^{-1} yr^{-1} in the 2000s) (Jia et al., 2014); and 7.4 kg N ha^{-1} yr^{-1} (from 12.64 kg N ha^{-1} yr^{-1} in the 1960s to 20.07 kg N ha^{-1} yr^{-1} in the 2000s) (Lu and Tian, 2014). Enhanced N deposition has changed the structure and function of terrestrial, aquatic and coastal ecosystems in China (Liu et al., 2011). To accurately estimate the N deposition in China, several monitoring networks have been established at the regional scale, e.g. in northern China (Pan et al., 2012), in forest ecosystems along the North–South Transect of Eastern China (NSTEC; based on the ChinaFLUX network) (Sheng et al., 2013), and in subtropical forest ecosystems in South China (Chen and Mulder, 2007). However, there are few observation sites

distributed in western China, particularly on the Tibetan Plateau (TP), resulting in uncertainty regarding the N deposition for China as a whole (Jia et al., 2014; X. J. Liu et al., 2013; Lu and Tian, 2014).

The TP covers an area of about 2.57 million km^2, occupying approximately 1/4 of the land area of China (Zhang et al., 2002). On the TP, alpine ecosystems are widely distributed and are sensitive to elevated N deposition. Multi-level N fertilization experiments have shown that alpine grassland ecosystems are N limited and have potential capacity to absorb increased N deposition (Y. W. Liu et al., 2013; Xu et al., 2014). However, long-term N addition can decrease the species richness of both vegetation and soil seed banks in alpine meadow ecosystems on the TP (Ma et al., 2014). Ice core records show that the inorganic N deposition on the TP has increased during recent decades (Hou et al., 2003; Kang et al., 2002a, b; Thompson et al., 2000; Zhao et al., 2011; Zheng et al., 2010), and this trend is also apparent in sediment cores of alpine lakes in the western and southeastern TP (Choudhary et al., 2013; Hu et al., 2014). To recognize the characteristics of ion deposition on the TP, a number of observations of precipitation chemistry have been carried out in the eastern TP in recent years (Jia, 2008; Tang et al., 2000; Zhang et al., 2003; N. N. Zhang et al., 2012). Nevertheless, in the western TP, observation sites are scarce, indicating that the situation in terms of N deposition across the entire TP remains unclear.

To quantitatively estimate the inorganic N wet deposition on the TP, we investigated the precipitation chemistry characteristics at five remote sites, situated mainly on the central and western TP. The sites are part of the Tibetan Observation and Research Platform (TORP) network (Ma et al., 2008). Specifically, our aims were to (1) clarify the amount of inorganic N wet deposition on the central and

western TP, and (2) assess the amount of inorganic N wet deposition for the entire TP by combining site-scale *in situ* measurements with those in previous studies.

2 Materials and methods

2.1 Precipitation sampling and chemical analysis

Using the Tibetan Observation and Research Platform (TORP) network (Ma et al., 2008), precipitation chemistry observations were conducted at five sampling sites: Southeast Tibet Station, Nam Co Station, Qomolangma Station, Ngari Station, and Muztagh Ata Station (Fig. 1), situated from the eastern to western TP and covering various climatic zones and vegetation types. A brief description of the five sites is shown in Table1.

During 2011–2013, we collected precipitation samples at each site, lasting at least one year. Precipitation samples were collected following each precipitation event, using an inner removable high-density polyethylene (HDPE) plastic bag in a pre-cleaned HDPE bucket. The HDPE bucket was placed 1.5 m above the ground. We opened the plastic bag at the beginning of the precipitation event, and collected precipitation samples at the end of the precipitation process. Then, the samples were transferred into pre-cleaned HDPE bottles (50 mL). Snowfall samples were melted at room temperature before being transferred into the HDPE bottles. All samples were kept frozen at the station and during transport until analysis in the laboratory. A total of 259 precipitation samples were collected, among which eight samples were abandoned due to breakage during transportation or the samples volume being less than 10 mL.

We analyzed the chemical composition of all precipitation samplings at the State Key Laboratory of Environmental Aquatic Chemistry, Research Center for Eco-Environmental Sciences, Chinese Academy of Sciences. Analyzed ions included NO_3^-, Cl^-, SO_4^{2-}, NH_4^+, Na^+, K^+, Ca^{2+} and Mg^{2+}. All ions were analyzed by the Ion Chromatography of Dionex-ICS2100. Samples for cation analysis were eluted on a Dionex 4-mm CS12A separatory column using 20 mM Methanesulfoni acid solution for an eluent pumped with a flow rate of 1.0 mL min^{-1}. Suppression was provided by a Dionex CSRS300 suppressor in recycle mode. For anion analysis, an IonPac AS19-HC column, 25 mM NaOH eluent and ASRS300 suppresser were used. The analytical detection limit was 2 ng g^{-1} for all ions.

2.2 Data quality control

Previously documented methods (Rodhe and Granat, 1984;Safai et al., 2004) were used for quality assurance and quality control purposes, resulting in six (2.4%) samples, which fell outside the range ($m-3\delta$, $m+3\delta$), being excluded. Here, m is the mean value and δ is the standard deviation. The Pearson correlation between Σ_{anions} and $\Sigma_{cations}$ was 0.82 ($p < 0.001$), suggesting credible data quality. The ratio of total anions to total cations was calculated following Eq. (1),

$$\frac{\sum \text{anions}}{\sum \text{cations}} = \frac{\sum_{k=1}^{n}(NO_3^- + Cl^- + SO_4^{2-})}{\sum_{k=1}^{n}(NH_4^+ + Na^+ + K^+ + Ca^{2+} + Mg^{2+})}, \quad (1)$$

where n is the number of samples. The ratio of ($\Sigma_{anions}/\Sigma_{cations}$) was 0.26, indicating that at least one major anion was not measured (C. Li et al., 2007). Considering that pH is alkaline in both precipitation and the surface soil layer (Ding et al., 2004; Y. H. Yang et al., 2012), the unmeasured anion was likely HCO_3^- (C. Li et al., 2007).

2.3 Statistical Analysis

For each site, consecutive samples in one year were selected to analyze the annual mean values of ions. The sampling times of the samples used at the five sites were as follows: Southeast Tibet Station, November 2011 to October 2012; Nam Co Station, August 2011 to July 2012; Qomolangma Station, April 2011 to March 2012; Ngari Station, January 2013 to December 2013; Muztagh Ata Station, January 2011 to December 2011. A total of 168 precipitation samples were selected, among which the number of samples for Southeast Tibet Station, Nam Co Station, Qomolangma Station, Ngari Station and Muztagh Ata Station was 53, 27, 30, 39 and 19, respectively.

The annual average ion concentration was calculated as the volume-weighted mean (VWM) following Eq. (2),

$$C = \frac{\sum_{i=1}^{n}(C_i \times P_i)}{\sum_{i=1}^{n} P_i}, \quad (2)$$

where C is the annual average ion concentration (μeq L^{-1}), C_i is the ion concentration of an individual sample i (μeq L^{-1}), and P_i is the precipitation amount corresponding to the sample i (mm).

Wet deposition of atmospheric N was calculated following Eq. (3),

$$N_{\text{wet}} = 0.00014 \times C_{\text{N}} \times P_{\text{annual}}, \quad (3)$$

where N_{wet} is the annual wet deposition of atmospheric inorganic N (NH_4^+-N or NO_3^--N, kg N ha^{-1} yr^{-1}), C_N is the annual average equivalent concentration of N (NH_4^+-N or NO_3^--N, μeq L^{-1}), P_{annual} is annual precipitation (mm yr^{-1}), and 0.00014 is the shift coefficient for the unit of μeq L^{-1} × mm yr^{-1} to the unit of kg N ha^{-1} yr^{-1}. Here, 1 μeq NH_4^+-N or NO_3^--N contains 1 μmol N, and the weight of 1 μmol N is 14×10^{-9} kg. Thus, μeq L^{-1} × mm yr^{-1} = 14×10^{-9} kg N × 10^3 m^{-3} × 10^{-3} m yr^{-1} = 14×10^{-9} kg N × 10^4 ha^{-1} yr^{-1} = 0.00014 kg N ha^{-1} yr^{-1}.

2.4 Source assessment of ion wet deposition

2.4.1 Enrichment factor

Enrichment factor (EF) has been widely used to examine the source contributions of major ions wet deposition in previous studies (Cao et al., 2009; Chabas and Lefevre, 2000; Kulshrestha et al., 1996; Lu et al., 2011; Okay et al., 2002; Shen et al., 2013; Xiao et al., 2013; Zhang et al., 2007). Commonly, Na is considered as the best reference element for seawater, due to its almost purely marine origin (Keene et al., 1986; Kulshrestha et al., 2003). Another element, Ca is normally used as a reference element for continental crust, because Ca is a typical lithophile element and its composition in soil barely changes (Zhang et al., 2007). In this study, Na and Ca were also used as reference element for seawater and continental crust, respectively.

On the TP, multiple lines of evidence demonstrate that Na^+ in precipitation on the TP mainly comes from oceans. Balestrini et al. (2014) monitored the chemical and isotopic compositions of precipitations at the Pyramid International Laboratory (5050m a.s.l.) on the southern slope of the Himalayas, and data analysis suggested that Na^+ and Cl^- were derived from the long-range transport of marine aerosols. Ice records in the central Himalayas show that Cl^-/Na^+ was positively related with the monsoon rainfall in northeast India, and there was a teleconnection between the Na^+ and Cl^- concentrations and the North Atlantic Oscillation, indicating Na^+ in the ice core mainly came from oceans (Wang et al., 2002). Na^+ has been used as a marine tracer when analyze the source contributions of ions wet deposition on the northeastern TP (Li et al., 2015), the southeastern TP (B. Liu et al., 2013) and the southern slope of central Himalayas (Tripathee et al., 2014).

On the TP, sandy desertification land covers about 3.1×10^5 km^2, accounting for 14% of the whole plateau, of which moderate sandy desertification land occupies 55.44% (Liu et al., 2005). The TP was regarded as an important dust source region (Fang et al., 2004; Han et al., 2009; Han et al., 2008). The TP dust sources contribute 69% of dust at the surface and 40% of dust in the lower troposphere on the TP (Mao et al., 2013). Moreover, arid regions are widely distributed surrounding the TP, e.g. central Asia, deserts of western China. The dust on the TP partly comes from the adjacent dust source regions, e.g. Taklimakan Desert in western China (Huang et al., 2007; Xia et al., 2008). Atmospheric dust aerosols over the TP are strongly impacted by local sources and enriched with Ca (Zhang et al., 2001). These dust aerosols in the atmosphere can interact with clouds and precipitation (Huang et al., 2014), and deposit on the surface with precipitation. Thus, Ca^{2+} is commonly used as a proxy of dust for ice core studies in the TP (Kang et al., 2002a; Kang et al., 2010; Kaspari et al., 2007; Wang et al., 2008). As a dust proxy, Ca^{2+} record in an ice core from the central TP even was significantly related regional zonal wind (westerlies) trends, and reflected the long-term control of regional atmospheric circulation strength over atmospheric dust concentrations (Grigholm et al., 2015). In addition, Ca also has been used as a reference element for continental crust when assess source of ion wet deposition in precipitation on the northern TP (Li et al., 2015).

In this study, the EF of an ion in precipitation relative to the ion in sea was estimated using Na as a reference element following Eq. (4),

$$\mathrm{EF}_{\mathrm{sea}} = \frac{[X/\mathrm{Na}^+]_{\mathrm{rain}}}{[X/\mathrm{Na}^+]_{\mathrm{sea}}}, \quad (4)$$

where EF_{sea} is the EF of an ion in precipitation relative to the ion in sea, X is an ion in precipitation, $[X/Na^+]_{rain}$ is the ratio from precipitation composition (μeq X / μeq Na^+), and $[X/Na^+]_{sea}$ is the ratio from sea composition (Keene et al., 1986; Turekian, 1968) (μeq X / μeq Na^+).

The EF of an element in precipitation relative to the element in soil was estimated using Ca as a reference element following Eq. (5),

$$\mathrm{EF_{soil}} = \frac{[X/\mathrm{Ca^{2+}}]_{\mathrm{rain}}}{[X/\mathrm{Ca^{2+}}]_{\mathrm{soil}}}, \quad (5)$$

where EF_{soil} is the EF of an element in precipitation relative to the element in soil, X is an ion in precipitation, $[X/Ca^{2+}]_{soil}$ is the ratio from precipitation composition (μg X / μg Ca^{2+}), and $[X/Ca^{2+}]_{soil}$ is the ratio from soil composition (Taylor, 1964) (μg X / μg Ca^{2+}).

To estimate fractions of marine, crustal and anthropogenic contributed to ions in precipitation, we calculated the sources of ionic components in precipitation using equations from previous studies (Cao et al., 2009; Lu et al., 2011; Zhang et al., 2007) as follows:

$$\mathrm{SSF}\ (\%) = \frac{[X/\mathrm{Na^+}]_{\mathrm{sea}}}{[X/\mathrm{Na^+}]_{\mathrm{rain}}} \times 100, \quad (6)$$

$$\mathrm{CF}\ (\%) = \frac{[X/\mathrm{Ca^{2+}}]_{\mathrm{soil}}}{[X/\mathrm{Ca^{2+}}]_{\mathrm{rain}}} \times 100, \quad (7)$$

$$\mathrm{AF}\ (\%) = 100 - \mathrm{SSF} - \mathrm{CF}, \quad (8)$$

where SSF is sea salt fraction, CF is crust fraction, and AF is anthropogenic fraction. Note that if SSF is greater than 1, SSF is recalculated as the difference between 1 and CF, and if CF is greater than 1, CF is recalculated as the difference between 1 and SSF.

2.4.2 Principal component analysis

Principal component analysis has been widely used in precipitation chemical studies to determine the effect of natural and anthropogenic sources on chemical composition of precipitation (Balasubramanian et al., 2001; Cao et al., 2009; Migliavacca et al., 2005; Zhang et al., 2007). In this study, principal component analysis was also used to examine the various source of major ions in precipitation at the five remote sites on the TP. Varimax-rotated principal component analysis was performed using "principal" function in package "psych" of R 3.2.0 (R Core Team, 2015; http://www.R-project.org).

2.4.3 Backward trajectory analysis

To identify the long range transport of water-soluble ions in precipitation, seven-day backward trajectories arriving at the sampling sites for each individual precipitation event were calculated. Backward trajectories were calculated using TrajStat (version 1.4.4R4, http://www.meteothinker.com/TrajStatProduct.html), which is a Geographic Information System based software, including a trajectory calculation module of HYSPLIT (Hybrid Single Particle Lagrangian Integrated Trajectory Model; http://www.arl.noaa.gov/ready/hysplit4.html) (Wang et al., 2009). The input meteorological data was the Global Data Assimilation System (GDAS) meteorological data archives of the Air Resource Laboratory, National Oceanic and Atmospheric Administration (NOAA) (ftp://arlftp.arlhq.noaa.gov/pub/archives/gdas1). All backward trajectories were calculated at 6-h interval (00:00, 06:00, 12:00, 18:00 UTC) at each sampling day, with an arrival height of 500 m above the ground. Then, cluster analysis was performed using of the trajectories during the one year-round sampling period at each site using TrajStat (version 1.4.4R4).

3 Results

3.1 Chemical composition of atmospheric precipitation

Figure 2 shows the seasonal dynamics of ion concentrations in precipitation at the five remote sites on the TP. Wet deposition of all ions mainly occurs in summer at all sites. Compared to the sites with relatively higher precipitation amounts, e.g. Ngari Station and Muztagh Ata Station, the sites with relatively lower precipitation amounts had relatively higher ion concentrations, e.g. Southeast Tibet Station and Nam Co Station (Fig. 2, Table 2). Ca^{2+} had the highest annual VWM concentration in precipitation at most sites (except for Nam Co Station), with the highest proportion accounting for measured ions of 54.6% at Southeast Tibet Station (Fig. 2 and 3). At Nam Co Station, NH_4^+ in precipitation had the highest proportion accounting for measured ions of 39.5%, higher than those at the other sites (ranging 12.9% at Southeast Tibet Station to 18.9% at Muztagh Ata Station) (Fig. 3). Compared to NH_4^+, NO_3^- had much lower proportion accounting for measured ions in precipitation, ranging 0.6% at Qomolangma Station to 14% at Nam Co Station (Fig. 3). The order of the average VWM of ion deposition at the five stations was: $Ca^{2+} > NH_4^+ > SO_4^{2-} > Cl^- > Na^+ > Mg^{2+} > NO_3^- > K^+$ (Table 2). All major ion concentrations in precipitation on the TP were much lower than those in northern and southern China (Table 2).

3.2 Wet deposition of atmospheric inorganic N

At Southeast Tibet Station, Nam Co Station, Qomolangma Station, Ngari Station, and Muztagh Ata Station, the NH_4^+-N wet deposition was 0.63, 0.68, 0.92, 0.36 and 1.25 kg N ha^{-1} yr^{-1}, respectively; the NO_3^--N wet deposition was 0.28, 0.24, 0.03, 0.08 and 0.3 kg N ha^{-1} yr^{-1}, respectively; and the inorganic N deposition was 0.91, 0.92, 0.94, 0.44 and 1.55 kg N ha^{-1} yr^{-1}, respectively (Table 3).

Besides the above five sites of the TORP network, previous site-scale *in situ* measurements of inorganic N wet deposition at other sites on the TP were also collected, e.g. at Waliguan (Tang et al., 2000), Wudaoliang (Yang et al., 1991), Lhasa (Zhang et al., 2003), Naidong (Jia, 2008), Biru (Jia, 2008), Jiangda (Jia, 2008), and Lijiang (N. N. Zhang et al., 2012). Combining site-scale *in situ* measurements in our study with those in previous studies, the average wet deposition of atmospheric NH_4^+-N, NO_3^--N and inorganic N on the TP were estimated to be 1.09, 0.57 and 1.66 kg N ha^{-1} yr^{-1}, respectively, and the estimated NH_4^+-N:NO_3^--N ratio in precipitation on the TP was 2:1. Both NH_4^+-N and NO_3^--N wet deposition on the TP were much lower than those in northern and southern China (Table 3).

3.3 Seasonal dynamics of inorganic N wet deposition

The inorganic N wet deposition mainly occurred as the form of NH_4^+-N during the summer at all sites (Fig. 4). Both concentrations of NH_4^+ and NO_3^- did not exhibited any clear seasonal pattern (Fig. 2). The seasonal dynamics inorganic N wet deposition at most stations appeared the shape of single peak type (Fig. 4). The seasonal pattern of inorganic N wet deposition were similar to the seasonal pattern of precipitation, rather than that of NH_4^+ or NO_3^- concentration (Fig. 2).

3.4 Source assessment of wet deposition of inorganic N and other ions

3.4.1 Enrichment factors

Table 4 shows the EFs of precipitation constituents at the five sites relative to seawater and soil. If the EF value of an ion in precipitation is much higher (lower) than 1, the ion is considered to be enriched (diluted) relative to the reference source. Among the five sites, Cl^- had a relatively lower EF_{sea} value,

ranging from 0.50 (Nam Co Station) to 0.90 (Qomolangma Station), but a relatively higher EF_{soil} value, ranging from 42.4 (Muztagh Ata Station) to 286 (Qomolangma Station). Different from Cl^-, NH_4^+ in precipitation was enriched relative to both marine origin and soil reference source at all sites, because its EF_{sea} values ranged from 11629 to 80684, and its EF_{soil} from 350 to 2378. Similar to NH_4^+, NO_3^- also had a relatively high value of both EF_{sea} and EF_{soil} at all five sites.

Table 5 shows the source contributions for major ions in precipitation of the five remote sites in this study. Almost all Cl^- and Na^+ in precipitation on the TP appeared to be of marine origin, with SSF value above 95% at the five sites. Nearly all Ca^{2+} in precipitation came from crust at the five sites, with the CF value being above 90%. Among the five sites, anthropogenic sources contributed at least 99% of NH_4^+ in precipitation, and NO_3^- in precipitation was also mainly influenced by anthropogenic activities, with AF values ranging from 95.3% to 99.9%.

3.4.2 Principal component analysis

Table 6 shows the 1st, 2nd and 3rd component of principal component analysis, which account for at least 85% of the total variance across the five sites. Na^+ and Cl^- were mainly explained by the same component at all sites. Principal component analysis shows that the variances of Ca^{2+} and Na^+ were represented by different components at four of five sites (except Southeast Tibet Station) (Table 6). The common variance of Ca^{2+}, Mg^{2+} and SO_4^{2-} as 1st component represents the largest proportion of the total specie variation at the 3 sites (Nam Co Station, Ngari Station and Muztagh Ata Station) in the central and western TP (Table 6). At Qomolangma Station, Na^+, Cl^-, K^+ and NH_4^+ as 1st component represents the largest proportion of the total specie variation (Table 6). Except for Qomolangma Station, at the other four sites, the variances of NH_4^+ were mainly represented by 3rd component (Table 6). At

Southeast Tibet Station, both Ca^{2+} and Na^{+} variances were mostly represented by the 1st component, but NO_3^- variances were mainly represented by the 2nd component (Table 6). At Nam Co Station, Qomolangma Station and Ngari Station, NO_3^- variances were mainly represented by the 3nd component, which were different with that of both Ca^{2+} and Na^{+} (Table 6). However, NO_3^- variances were mainly represented by the 1st component at Muztagh Ata Station (Table 6).

3.4.3 Backward trajectory analysis

Fig. 5 shows the seven-day backward trajectories of air mass arriving at the five remote sites at the sampling days. The transport pathways of air masses were various with the different sites (Fig. 5). The cluster trajectory results showed that at Muztagh Ata Station, nearly all air masses at sampling days were transported from Central Asia and Middle East (Fig. 5a). Different to Muztagh Ata Station, almost all air masses at Nam Co Station were transported from South Asia (Fig. 5d). For Ngari Station, Qomolangma Station, and Southeast Tibet Station, the air masses at sampling days were mainly transported from South Asia, with the proportion of 90%, 79.8% and 90.6%, respectively (Figs. 5b-5e). Besides South Asia, Central Asia, Qaidam Basin and Middle East was the second source of air masses at sampling days for Ngari Station, Qomolangma Station, and Southeast Tibet Station, respectively (Figs. 5b-5e).

4 Discussion

4.1 Wet deposition of atmospheric inorganic N on the TP

According to our field observations, wet deposition of atmospheric inorganic N on the western TP was lower than that on the eastern TP. For example, the rates of inorganic N wet deposition at Ngari Station

and Muztagh Ata Station, located on the western TP, were 0.44 and 1.55 kg N ha^{-1} yr^{-1}, respectively, which were lower than those at the stations on the eastern TP, e.g. Jiangda (1.91 kg N ha^{-1} yr^{-1}), Lijiang (1.89 kg N ha^{-1} yr^{-1}) and Waliguan (2.92 kg N ha^{-1} yr^{-1}) (Table 3). However, the concentrations of inorganic N in precipitation at the sites on the western TP were comparable to those at the sites on the eastern TP. For instance, the annual average concentrations of NH_4^+ in precipitation at Ngari Station and Muztagh Ata Station were 20.5 and 42.0 μeq L^{-1}, respectively, which were higher than those at stations on the eastern TP, e.g. Lijiang (11.4 μeq L^{-1}) and Lhasa (14.3 μeq L^{-1}) (Table 2). Meanwhile, compared to Lijiang and Lhasa, Ngari Station and Muztagh Ata had lower annual precipitation rates of 124.6 and 213.6 mm yr^{-1} (Table 2). Therefore, compared to the eastern TP, the western TP had relatively lower inorganic N deposition, probably due to its lower precipitation rather than its comparable inorganic N concentration in precipitation.

Wet deposition of inorganic N for the entire TP was much lower than that in northern and southern China (Table 3). The average wet deposition of atmospheric inorganic N (sum of NH_4^+-N and NO_3^+-N) for the TP was estimated to be 1.66 kg N ha^{-1} yr^{-1}. This was much lower than the inorganic N wet deposition in the cities of both northern and southern China, e.g. Beijing, Tianjin, Tangshan, Dalian, Nanjing, Hangzhou, Ningbo, Shanghai, Shenzhen and Guiyang (Table 3). Moreover, the inorganic N wet deposition on the TP was also lower than that in the forest ecosystems of eastern China, e.g. TieShanPing, LiuChongGuan, LeiGongShan, CaiJiaTang and XiLiuHe (Table 3). Overall, compared to eastern China, the TP had relatively lower inorganic N wet deposition, probably due to following two reasons. First, except for Southeast Tibet Station and Lijiang, most N observation sites on the TP are located in typical arid and semi-arid regions, with annual precipitation ranging from 124.6 mm yr^{-1} at Ngari Station to 582 mm yr^{-1} at Biru. Compared to this, annual precipitation rates at sites in eastern

China are much higher, particularly in southern China, where annual precipitation ranges from 825.5 mm yr^{-1} at Shanghai to 1769 mm yr^{-1} at Shenzhen (Table 3). Second, the average annual concentration of inorganic N (NH_4^+-N, NO_3^--N) in precipitation on the TP was much lower than that in eastern China, especially at cities in northern China (Table 2). This is probably because the effects of anthropogenic activities in eastern China are much more intense than on the TP, which is referred to as "The Third Pole" and has an average altitude exceeding 4,000 meters above sea level (Qiu, 2008; Yao et al., 2012).

4.2 Source assessment of atmospheric inorganic N wet deposition on the TP

To analyze the source contributions of major ions wet deposition, EF was applied using Na and Ca as reference element for seawater and continental crust, respectively. Here, Na and Ca in precipitation on the TP was hypothesized mainly coming seawater and continental crust, respectively. This assumption was partly confirmed by the results of principal component analysis in this study (Table 6). Principal component analysis shows that the variances of Ca^{2+} and Na^+ were represented by different components at four of five sites (except Southeast Tibet Station), indicating different source of Ca^{2+} and Na^+ in precipitation on the TP (Table 6). Moreover, Na^+ and Cl^- were mainly explained by the same component at all sites. This indicates that Na^+ and Cl^- were likely contributed by the same source: sea-salt (Table 6). This assumption was also confirmed by the relatively high Pearson correlation between Na^+ and Cl^- at all five sites (Table S1 in the supplementary material). At Southeast Tibet Station, both Ca^{2+} and Na^+ variances were mostly represented by the 1st component (Table 6). This probably because South Asia is also an important source of dust aerosols in the southeastern TP during the during the monsoon period (Zhao et al., 2013).

EF analysis results showed that at all the five sites, both NH_4^+ and NO_3^- in precipitation were mainly contributed by anthropogenic sources (Table 5). This was also confirmed by principal component analysis. Different with Ca^{2+} and Na^+, NH_4^+ variances were mainly represented by 3rd component at four in five sites (except for Qomolangma Station) (Table 6). Except for Muztagh Ata Station, at the other four stations, NO_3^- variances were also represented by different component with that of Ca^{2+} and Na^+ variances (Table 6). This indicates that the source of inorganic N wet deposition was probably different with the sources of Ca^{2+} or Na^+. Meanwhile, at all five sites, Na and Ca mainly came from seawater and continental crust, respectively. Therefore, inorganic N wet deposition at the five sites on the TP was mainly influenced by anthropogenic activities.

TP is mainly controlled by westerlies and Indian monsoon (Yao et al., 2013). The northern TP is mainly influenced by westerlies, and the southern TP is mainly controlled by the Indian monsoon in summer seasons, but by the westerlies during non-monsoon seasons (Yao et al., 2013). N emissions from anthropogenic activities in Central Asia might be transported to the northern TP by westerlies. N emissions from anthropogenic activities in South Asia (e.g. India) might be transported to the southern TP by Indian monsoon. After China and USA, India has been the third largest producer and consumer of fertilizers due to intensification of agriculture, resulting in high anthropogenic N emissions (Aneja et al., 2012). At present, reactive N emissions from crop and livestock farming in India were second only to that in China (Aneja et al., 2012). For instance, ammonia (NH_3) emissions from livestock and fertilizer applications in India in 2003 was estimated as 1705 Gg yr^{-1} and 1697 Gg yr^{-1}, respectively (Aneja et al., 2012). Moreover, in India, field burning of crop residue (FBCR) is another critical anthropogenic activity leading to N emissions. N emissions in India due to FBCR showed increase trend in the past 3 decades (Sahai et al., 2011). In 2010, 6300 Gg of dry biomass are estimated to be

subjected to FBCR in India, resulting in 350 Gg N emissions (Sahai et al., 2011). Besides Indian monsoon, biomass-burning emissions in South Asia could be across the Himalayas and transported to the TP by the mountain/valley wind (Cong et al., 2015).

We applied backward trajectory analysis to identify the long range transport of atmospheric inorganic N wet deposition at the five sites on the TP (Fig. 5). There is large spatial heterogeneity of air mass transport pathways across the five sites. At Muztagh Ata Station, wet deposition was mainly transported from Central Asia and Middle East (Fig. 5a). It seems that air mass from South Asia has no influence on the wet deposition at Muztagh Ata Station. This is probably because Muztagh Ata Station is located on the northwestern TP, where is almost completely controlled by westerlies, rather than Indian Monsoon (Yao et al., 2013). Thus, anthropogenic activities in Central Asia and Middle East are the principal source of the inorganic N wet deposition at Muztagh Ata Station. Except for Muztagh Ata Station, inorganic N wet deposition at the other four sites was mainly influenced by anthropogenic activities in South Asia and was probably transported by India Monsoon (Figs. 5b-5e). At Ngari Station, 90.0% of wet deposition was transported from Nepal and North India through Indian Monsoon, and 10.0% wet deposition was transported from Central Asia and Qaidam Basin through westerlies (Fig. 5b). At Qomolangma Station and Nam Co Station, inorganic N wet deposition was mainly influenced by the anthropogenic activities in the northeastern India and Bangladesh (Figs. 5c and 5d). At Southeast Tibet Station, 90.6% of wet deposition was transported from India, Bangladesh and Myanmar by India Monsoon, and the other 9.4% came from the western TP and Middle East (Fig. 5e).

4.3 Comparison of inorganic N wet deposition on the TP with previous estimations

Long-term dataset series of N deposition have been established based on observations (Lu and Tian, 2007, 2014, 2015) or model simulations (Dentener et al., 2006). These datasets have been used to estimate global or regional N deposition (Dentener et al., 2006; Lu and Tian, 2007) and drive ecosystem models to examine the ecological effects of elevated N deposition (Lu and Tian, 2013). Thus, reliable N deposition datasets are a prerequisite for N deposition estimation or driving ecosystem models. Here, the estimation of N wet deposition on the TP based on our field observations is compared with previous estimations via limited observations or simulations.

Lu and Tian (2007) estimated the inorganic N wet deposition as ranging from 4.16 kg N ha^{-1} yr^{-1} in Tibet Autonomous Region (on the western TP) to 4.76 kg N ha^{-1} yr^{-1} in Qinghai Province (on the eastern TP). Recently, Jia et al. (2014) estimated the inorganic N wet deposition during the 2000s as ranging from 6.11 kg N ha^{-1} yr^{-1} in Tibet Autonomous Region to 7.87 kg N ha^{-1} yr^{-1} in Qinghai Province. Those estimations were much higher even than the highest record of inorganic N wet deposition observations on the TP (3.08 kg N ha^{-1} yr^{-1} at Biru during 2006-2007) (Table 3). In this study, combing *in situ* measurements at 5 sites in this study and 7 sites in previous studies (Table 2), the average wet deposition of atmospheric NH_4^+-N, NO_3^+-N and inorganic N on the TP were estimated to be 1.09, 0.57 and 1.66 kg N ha^{-1} yr^{-1}, respectively. According to our study, both Lu and Tian (2007) and Jia et al. (2014) highly overestimated inorganic N wet deposition on the TP, probably due to following two reasons. First, the observations used in previous regional-scale estimations were limited, with fewer observation sites than used in the present study. For example, there were only four sites in Tibet Autonomous Region and one site in Qinghai Province used in the estimation of Jia et al. (2014). Such limited observations lead to uncertainty in the conclusions drawn regarding inorganic N wet deposition on the entire TP. Second, the Kriging interpolation technique was used in both Lu and Tian

412 (2007) and Jia et al. (2014) to estimate the spatial pattern of inorganic N wet deposition in China.
413 However, observation sites are sparsely distributed on the TP, and the estimation of inorganic N wet
414 deposition is largely influenced by N deposition observations in the surrounding regions of much lower
415 altitude. The average altitude of the TP is above 4000 m, where both the climate and anthropogenic
416 activities are substantially different with those in lower altitude areas. For example, the average
417 inorganic N wet deposition was 1.66 kg N ha^{-1} yr^{-1}, which was much lower than that in northern and
418 southern China (Table 3). The interpolations at the national scale in Lu and Tian (2007) and Jia et al.
419 (2014) probably overestimated inorganic N wet deposition on the TP. In addition, we also estimated
420 the inorganic N wet deposition for the entire TP using Kriging interpolation, but only based on the site-
421 scale *in situ* measurements on the TP (12 sites, including: 5 sites in this study and 7 sites in previous
422 field observations), rather than the observations in the surrounding regions of much lower altitude. The
423 inorganic N wet deposition for the entire TP estimation based on the Kriging interpolation in our study
424 is 1.76 kg N ha^{-1} yr^{-1} (Fig. S1 and spatial data as NetCDF file in the supplementary material), which is
425 much lower than that in previous interpolation studies (Lu and Tian, 2007; Jia et al., 2014), but is
426 comparable with the averaged inorganic N wet deposition among the 12 sites (1.66 kg N ha^{-1} yr^{-1})
427 (Table 2).

428 Atmospheric chemistry transport models are commonly used to calculate current and future N
429 deposition. Dentener et al. (2006) used 23 atmospheric chemistry transport models to assess both
430 global and regional N deposition. Compared to observation records, Dentener et al. (2006)
431 underestimated inorganic N wet deposition over the whole of China (Lu and Tian, 2007), but
432 overestimated it for the TP. According to Dentener et al. (2006), the NH_4^+, NO_3^- and inorganic N wet
433 deposition on the TP are 1.97, 0.99 and 2.96 kg N ha^{-1} yr^{-1}, respectively—nearly double that of N

deposition estimated in our study. Based on site-scale *in situ* measurements, we provide a more accurate regional-scale estimation of inorganic N wet deposition on the TP, which can be used as background information in research focusing on the responses of alpine ecosystems to elevated N deposition. Besides assessment of N deposition, N deposition simulated by atmospheric chemistry transport models is usually used to drive large-scale ecosystem models for integrated ecosystem assessment (Xu-Ri et al., 2012; Zaehle, 2013). The ecological effects of N addition are probably not only influenced by the quantity of N deposition, but also by the proportions of each component, e.g. the NH_4^+-N:NO_3^--N ratio. For example, in African savannas, plants demonstrate N uptake preference, which is likely influenced by the NH_4^+-N:NO_3^--N ratio in their native habitats (Wang and Macko, 2011). However, in most current N fertilization experiments, the N forms of fertilizer are NH_4NO_3, NH_4^+-N or NO_3^--N (Liu and Greaver, 2009), with the NH_4^+-N:NO_3^--N ratio of N wet deposition at experimental sites not considered. Our work shows that the estimated NH_4^+-N:NO_3^--N ratio of inorganic N wet deposition on the TP is 2:1, which is consistent with the modelled estimation of Dentener et al. (2006), but lower than the NH_4^+-N:NO_3^--N ratio of 2.5 in forest ecosystems in eastern China (Du et al., 2014). This NH_4^+-N:NO_3^--N ratio (2:1) is recommended to be considered when N fertilization experiments are conducted in alpine ecosystems on the TP.

4.4 Uncertainty and recommendations

Combining our *in situ* measurements at five remote sites and previous site-scale field observations, the inorganic N wet deposition on the TP was quantitatively assessed in this study. The assessment is conducive to accurately estimating N wet deposition for the entire nation of China, and provides background information of N wet deposition for the studies focusing on the alpine ecological effects of elevated N deposition. Despite this, there are uncertainties in the estimation of N deposition on the

TP due to following reasons. First, total N deposition comprises wet deposition (in the form of precipitation) and dry deposition (in the form of gases and particles). Considering the whole of China, dry deposition contributes 30% to total inorganic N deposition (Lu and Tian, 2007, 2014, 2015). In northern China, this ratio is much higher, at 60% (Pan et al., 2012). However, in this study, we only estimated the inorganic N wet deposition on the TP, with the situation regarding dry deposition remaining unclear. Thus, investigation of N dry deposition is critical for assessing total N deposition on the TP. Second, the TP covers an area of about 2.57 million km^2, occupying approximately 1/4 of the land area of China (Zhang et al., 2002). Precipitation on the TP is influenced by both the Indian monsoon and westerlies, leading to spatial variation in the origins of N wet deposition. Therefore, it is necessary to establish N wet deposition observation sites in different climatic zones. Third, besides spatial heterogeneity, N deposition on the TP also possesses temporal heterogeneity. Inorganic N wet deposition on the TP has increased during recent decades, as recorded in ice cores (Hou et al., 2003;Kang et al., 2002a, b;Thompson et al., 2000;Zhao et al., 2011;Zheng et al., 2010) and sediment cores of alpine lakes (Choudhary et al., 2013;Hu et al., 2014). The long-term trend and inter-annual variability of inorganic N wet deposition on the TP can't be quantitatively characterized by the short-term *in situ* measurements in this study. Overall, critical questions remain open regarding the quantitative understanding of N deposition on the TP. Therefore, to deepen our understanding N deposition on the TP, it is essential to perform long-term *in situ* measurements of N wet and dry deposition in various climate zones in the future.

5 Conclusion

Alpine ecosystems on the TP are sensitive to elevated N deposition, and the inorganic N deposition has been increasing since the mid-20th century. However, the amount of inorganic N wet deposition

on the Tibetan remains unclear, due to a paucity of *in situ* measurement. In this study, using stations in the TORP network, we conducted *in situ* measurements of major ions wet deposition at five remote sites, situated mainly on the central and western TP. Among the five sites, both NH_4^+-N and NO_3^--N were mainly contributed by anthropogenic sources. Combining site-scale *in situ* measurements in our and previous studies, the average wet deposition of atmospheric NH_4^+-N, NO_3^--N and inorganic N on the TP are estimated to be 1.09, 0.57 and 1.66 kg N ha^{-1} yr^{-1}, respectively. Considering the entire TP, according to our results, previous regional-scale assessment have highly overestimated inorganic N wet deposition, either through simulations with atmospheric chemistry transport models (Dentener et al., 2006) or interpolations based on limited field observations for the whole of China (Jia et al., 2014; Lu and Tian, 2007). The NH_4^+-N:NO_3^--N ratio in precipitation on the TP was found to be 2:1, which is consistent with model simulations (Dentener et al., 2006). To clarify the total N deposition on the TP more clearly, we recommend conducting long-term monitoring of both wet and dry deposition of N in various climate zones in the future work.

Acknowledgements

We are grateful to the staff at the Southeast Tibet Observation and Research Station for the Alpine Environment, Chinese Academy of Sciences (Southeast Tibet Station), Nam Co Monitoring and Research Station for Multisphere Interactions, Chinese Academy of Sciences (Nam Co Station), Qomolangma Atmospheric and Environmental Observation and Research Station, Chinese Academy of Sciences (Qomolangma Station), Ngari Desert Observation and Research Station (Ngari Station) and Muztagh Ata Westerly Observation and Research Station (Muztagh Ata Station) for their assistance in collecting the samples and providing the precipitation data. The authors also thank Da Wei, Dongxue Dai, Xiaodong Geng, Tenzin Tarchen and Shan Lu for their contributions to the field

work. This work was supported by the Strategic Priority Research Program—Climate Change: Carbon Budget and Related Issues, of the Chinese Academy of Sciences (XDA05050404-3-2, XDA05020402) and the National Natural Science Foundation of China (40605032, 40975096, 41175128).

References

Aneja, V. P., Schlesinger, W. H., Erisman, J. W., Behera, S. N., Sharma, M., and Battye, W.: Reactive nitrogen emissions from crop and livestock farming in India, Atmos. Environ., 47, 92-103, doi: 10.1016/j.atmosenv.2011.11.026, 2012.

Balasubramanian, R., Victor, T., and Chun, N.: Chemical and statistical analysis of precipitation in Singapore, Water. Air Soil Poll., 130, 451-456, doi: 10.1023/A:1013801805621, 2001.

Balestrini, R., Polesello, S., and Sacchi, E.: Chemistry and isotopic composition of precipitation and surface waters in Khumbu valley (Nepal Himalaya): N dynamics of high elevation basins, Sci. Total. Environ., 485, 681-692, doi: 10.1016/j.scitotenv.2014.03.096, 2014.

Basto, S., Thompson, K., Phoenix, G., Sloan, V., Leake, J., and Rees, M.: Long-term nitrogen deposition depletes grassland seed banks, Nat. Commun., 6, 6185, doi: 10.1038/ncomms7185, 2015.

Canfield, D. E., Glazer, A. N., and Falkowski, P. G.: The evolution and future of Earth's nitrogen cycle, Science, 330, 192-196, doi: 10.1126/science.1186120, 2010.

Cao, Y. Z., Wang, S. Y., Zhang, G., Luo, J. Y., and Lu, S. Y.: Chemical characteristics of wet precipitation at an urban site of Guangzhou, South China, Atmos. Res., 94, 462-469, doi: 10.1016/j.atmosres.2009.07.004, 2009.

Cong, Z. Y., Kawamura, K., Kang, S. C., and Fu, P. Q.: Penetration of biomass-burning emissions from South Asia through the Himalayas: new insights from atmospheric organic acids, Sci. Rep.-Uk,

5, 9580, doi: 10.1038/srep09580, 2015.

Chabas, A., and Lefevre, R. A.: Chemistry and microscopy of atmospheric particulates at Delos (Cyclades-Greece), Atmos. Environ., 34, 225-238, doi: 10.1016/S1352-2310(99)00255-1, 2000.

Chen, X. Y., and Mulder, J.: Atmospheric deposition of nitrogen at five subtropical forested sites in South China, Sci. Total. Environ., 378, 317-330, doi:10.1016/j.scitotenv.2007.02.028, 2007.

Choudhary, P., Routh, J., and Chakrapani, G. J.: A 100-year record of changes in organic matter characteristics and productivity in Lake Bhimtal in the Kumaon Himalaya, NW India, J. Paleolimnol., 49, 129-143, doi: 10.1007/s10933-012-9647-9, 2013.

Dentener, F., Drevet, J., Lamarque, J. F., Bey, I., Eickhout, B., Fiore, A. M., Hauglustaine, D., Horowitz, L. W., Krol, M., Kulshrestha, U. C., Lawrence, M., Galy-Lacaux, C., Rast, S., Shindell, D., Stevenson, D., Van Noije, T., Atherton, C., Bell, N., Bergman, D., Butler, T., Cofala, J., Collins, B., Doherty, R., Ellingsen, K., Galloway, J., Gauss, M., Montanaro, V., Muller, J. F., Pitari, G., Rodriguez, J., Sanderson, M., Solmon, F., Strahan, S., Schultz, M., Sudo, K., Szopa, S., and Wild, O.: Nitrogen and sulfur deposition on regional and global scales: A multimodel evaluation, Global Biogeochem. Cycles, 20, GB4003, doi: 10.1029/2005GB002672, 2006.

Ding, G. A., Xu, X. B., and Wang, S. F.: Database from the acid rain network of China meteorological administration and it's preliminary analyses, Journal of Applied Meteorological Science, 15, 85-94, 2004 (in Chinese with English abstract).

Ding, M., Yao, F., Chen, J., Wang, X., and Yang, S.: Chemical characteristics of acidic precipitation in Tiantong, Zhejiang Province, Acta Scientiae Circumstantiae, 32, 2245-2252, 2012 (in Chinese with English abstract).

Du, E., Jiang, Y., Fang, J. Y., and de Vries, W.: Inorganic nitrogen deposition in China's forests: Status and characteristics, Atmos. Environ., 98, 474-482, doi: 10.1016/j.atmosenv.2014.09.005, 2014.

545 Erisman, J. W., Galloway, J., Seitzinger, S., Bleeker, A., and Butterbach-Bahl, K.: Reactive nitrogen
546 in the environment and its effect on climate change, Curr. Opin. Env. Sust., 3, 281-290, doi:
547 10.1016/j.cosust.2011.08.012, 2011.
548 Erisman, J. W., Galloway, J. N., Seitzinger, S., Bleeker, A., Dise, N. B., Petrescu, A. M. R., Leach, A.
549 M., and de Vries, W.: Consequences of human modification of the global nitrogen cycle, Philos.
550 T. R. Soc. B, 368, 20130116, doi: 10.1098/rstb.2013.0116, 2013.
551 Fagerli, H., and Aas, W.: Trends of nitrogen in air and precipitation: Model results and observations at
552 EMEP sites in Europe, 1980-2003, Environ. Pollut., 154, 448-461, doi:
553 10.1016/j.envpol.2008.01.024, 2008.
554 Fang, X. M., Han, Y. X., Ma, J. H., Song, L. C., Yang, S. L., and Zhang, X. Y.: Dust storms and loess
555 accumulation on the Tibetan Plateau: A case study of dust event on 4 March 2003 in Lhasa,
556 Chinese Sci. Bull., 49, 953-960, doi: 10.1360/03wd0180, 2004.
557 Galloway, J. N., Townsend, A. R., Erisman, J. W., Bekunda, M., Cai, Z. C., Freney, J. R., Martinelli,
558 L. A., Seitzinger, S. P., and Sutton, M. A.: Transformation of the nitrogen cycle: Recent trends,
559 questions, and potential solutions, Science, 320, 889-892, doi: 10.1126/science.1136674, 2008.
560 Gao, J. G., Zhang, Y. L., Liu, L. S., and Wang, Z. F.: Climate change as the major driver of alpine
561 grasslands expansion and contraction: A case study in the Mt. Qomolangma (Everest) National
562 Nature Preserve, southern Tibetan Plateau, Quatern. Int., 336, 108-116, doi:
563 10.1016/j.quaint.2013.09.035, 2014.
564 Grigholm, B., Mayewski, P. A., Kang, S., Zhang, Y., Morgenstern, U., Schwikowski, M., Kaspari, S.,
565 Aizen, V., Aizen, E., Takeuchi, N., Maasch, K. A., Birkel, S., Handley, M., and Sneed, S.:
566 Twentieth century dust lows and the weakening of the westerly winds over the Tibetan Plateau,
567 Geophys. Res. Lett., 42, 2434-2441, doi: 10.1002/2015gl063217, 2015

568 Gruber, N., and Galloway, J. N.: An Earth-system perspective of the global nitrogen cycle, Nature, 451,
569 293-296, doi: 10.1038/nature06592, 2008.
570 Han, Y. X., Fang, X. M., Kang, S. C., Wang, H. J., and Kang, F. Q.: Shifts of dust source regions over
571 central Asia and the Tibetan Plateau: Connections with the Arctic oscillation and the westerly jet,
572 Atmos. Environ., 42, 2358-2368, doi: 10.1016/j.atmosenv.2007.12.025, 2008.
573 Han, Y. X., Fang, M., Zhao, T. L., Bai, H. Z., Kang, S. C., and Song, L. C.: Suppression of precipitation
574 by dust particles originated in the Tibetan Plateau, Atmos. Environ., 43, 568-574, doi:
575 10.1016/j.atmosenv.2008.10.018, 2009.
576 Hou, S.: Chemical Characteristics of Precipitation at the Headwaters of the Ürümqi River in the
577 Tianshan Mountains, Journal of Glaciology and Geocryology, 23, 80-84, 2001 (in Chinese with
578 English abstract).
579 Hou, S. G., Qin, D. H., Zhang, D. Q., Kang, S. C., Mayewski, P. A., and Wake, C. P.: A 154a high-
580 resolution ammonium record from the Rongbuk Glacier, north slope of Mt. Qomolangma
581 (Everest), Tibet-Himal region, Atmos. Environ., 37, 721-729, doi:10.1016/S1352-
582 2310(02)00582-4, 2003.
583 Hu, Z. J., Anderson, N. J., Yang, X. D., and McGowan, S.: Catchment-mediated atmospheric nitrogen
584 deposition drives ecological change in two alpine lakes in SE Tibet, Glob. Change Biol., 20, 1614-
585 1628, doi: 10.1111/Gcb.12435, 2014.
586 Huang, J. P., Minnis, P., Yi, Y. H., Tang, Q., Wang, X., Hu, Y. X., Liu, Z. Y., Ayers, K., Trepte, C., and
587 Winker, D.: Summer dust aerosols detected from CALIPSO over the Tibetan Plateau, Geophys.
588 Res. Lett., 34, L18805, doi: 10.1029/2007gl029938, 2007.
589 Huang, J. P., Wang, T. H., Wang, W. C., Li, Z. Q., and Yan, H. R.: Climate effects of dust aerosols over
590 East Asian arid and semiarid regions, J. Geophys. Res.-Atmos., 119, 11398-11416, doi:

591 10.1002/2014jd021796, 2014.
592 Huang, K., Zhuang, G. S., Xu, C., Wang, Y., and Tang, A. H.: The chemistry of the severe acidic
593 precipitation in Shanghai, China, Atmos. Res., 89, 149-160, doi: 10.1016/j.atmosres.2008.01.006,
594 2008.
595 Huang, Y. L., Wang, Y. L., and Zhang, L. P.: Long-term trend of chemical composition of wet
596 atmospheric precipitation during 1986-2006 at Shenzhen City, China, Atmos. Environ., 42, 3740-
597 3750, doi: 10.1016/j.atmosenv.2007.12.063, 2008.
598 Jia, J.: Study of atmospheric wet deposition of nitrogen in Tibetan Plateau, Master, Tibet University,
599 2008 (in Chinese with English abstract).
600 Jia, Y., Yu, G., He, N., Zhan, X., Fang, H., Sheng, W., Zuo, Y., Zhang, D., and Wang, Q.: Spatial and
601 decadal variations in inorganic nitrogen wet deposition in China induced by human activity, Sci.
602 Rep.-UK, 4, 3763, doi: 10.1038/srep03763, 2014.
603 Kang, S., Mayewski, P. A., Qin, D., Yan, Y., Hou, S., Zhang, D., Ren, J., and Kruetz, K.:
604 Glaciochemical records from a Mt. Everest ice core: relationship to atmospheric circulation over
605 Asia, Atmos. Environ., 36, 3351-3361, doi:10.1016/S1352-2310(02)00325-4, 2002a.
606 Kang, S. C., Mayewski, P. A., Qin, D. H., Yan, Y. P., Zhang, D. Q., Hou, S. G., and Ren, J. W.:
607 Twentieth century increase of atmospheric ammonia recorded in Mount Everest ice core, J.
608 Geophys. Res.-Atmos., 107, 4595, doi: 10.1029/2001jd001413, 2002b.
609 Kang, S. C., Zhang, Y. L., Zhang, Y. J., Grigholm, B., Kaspari, S., Qin, D. H., Ren, J. W., and Mayewski,
610 P.: Variability of atmospheric dust loading over the central Tibetan Plateau based on ice core
611 glaciochemistry, Atmos. Environ., 44, 2980-2989, doi: 10.1016/j.atmosenv.2010.05.014, 2010.
612 Kaspari, S., Mayewski, P., Kang, S., Sneed, S., Hou, S., Hooke, R., Kreutz, K., Introne, D., Handley,
613 M., Maasch, K., Qin, D., and Ren, J.: Reduction in northward incursions of the South Asian

monsoon since approximate to 1400 AD inferred from a Mt. Everest ice core, Geophys. Res. Lett., 34, L16701, doi: 10.1029/2007gl030440, 2007.

Keene, W. C., Pszenny, A. A. P., Galloway, J. N., and Hawley, M. E.: Sea-salt corrections and interpretation of constituent ratios in marine precipitation, J. Geophys. Res.-Atmos., 91, 6647-6658, doi: 10.1029/Jd091id06p06647, 1986.

Kulshrestha, U. C., Sarkar, A. K., Srivastava, S. S., and Parashar, D. C.: Investigation into atmospheric deposition through precipitation studies at New Delhi (India), Atmos. Environ., 30, 4149-4154, doi: 10.1016/1352-2310(96)00034-9, 1996.

Kulshrestha, U. C., Kulshrestha, M. J., Sekar, R., Sastry, G. S. R., and Vairamani, M.: Chemical characteristics of rainwater at an urban site of south-central India, Atmos. Environ., 37, 3019-3026, doi: 10.1016/S1352-2310(03)00266-8, 2003.

Lan, Z., Jenerette, G. D., Zhan, S., Li, W., Zheng, S., and Bai, Y.: Testing the scaling effects and mechanisms of N-induced biodiversity loss: Evidence from a decade-long grassland experiment, J. Ecol., doi: 10.1111/1365-2745.12395, 2015.

Lehmann, C. M. B., Bowersox, V. C., and Larson, S. M.: Spatial and temporal trends of precipitation chemistry in the United States, 1985-2002, Environ. Pollut., 135, 347-361, doi: 10.1016/j.envpol.2004.11.016, 2005.

Li, C., Kang, S. C., Zhang, Q. G., and Kaspari, S.: Major ionic composition of precipitation in the Nam Co region, Central Tibetan Plateau, Atmos. Res., 85, 351-360, doi:10.1016/j.atmosres.2007.02.006, 2007.

Li, M., Ma, Y., Ishikawa, H., Ma, W., Sun, F., Wang, Y., and Zhu, Z.: Characteristics of micrometeorological elements near surface and soil on the northern slope of Mt. Qomolangma area, Plateau Meteorology, 26, 1263-1268, 2007 (in Chinese with English abstract).

637 Li, Z. J., Li, Z. X., Wang, T. T., Gao, Y., Cheng, A. F., Guo, X. Y., Guo, R., Jia, B., Song, Y. X., Han,
638 C. T., and Theakstone, W.: Composition of wet deposition in the central Qilian Mountains, China,
639 Environ. Earth Sci., 73, 7315-7328, doi: 10.1007/s12665-014-3907-0, 2015.
640 Liu, B., Kang, S. C., Sun, J. M., Zhang, Y. L., Xu, R., Wang, Y. J., Liu, Y. W., and Cong, Z. Y.: Wet
641 precipitation chemistry at a high-altitude site (3,326 m a.s.l.) in the southeastern Tibetan Plateau,
642 Environ. Sci. Pollut. R., 20, 5013-5027, doi: 10.1007/s11356-012-1379-x, 2013.
643 Liu, L. L., and Greaver, T. L.: A review of nitrogen enrichment effects on three biogenic GHGs: the
644 CO_2 sink may be largely offset by stimulated N_2O and CH_4 emission, Ecol. Lett., 12, 1103-1117,
645 doi: 10.1111/j.1461-0248.2009.01351.x, 2009.
646 Liu, X. J., Duan, L., Mo, J. M., Du, E. Z., Shen, J. L., Lu, X. K., Zhang, Y., Zhou, X. B., He, C. N.,
647 and Zhang, F. S.: Nitrogen deposition and its ecological impact in China: An overview, Environ.
648 Pollut., 159, 2251-2264, doi: 10.1016/j.envpol.2010.08.002, 2011.
649 Liu, X. J., Zhang, Y., Han, W. X., Tang, A. H., Shen, J. L., Cui, Z. L., Vitousek, P., Erisman, J. W.,
650 Goulding, K., Christie, P., Fangmeier, A., and Zhang, F. S.: Enhanced nitrogen deposition over
651 China, Nature, 494, 459-462, doi: 10.1038/nature11917, 2013.
652 Liu, Y. H., Dong, G. R., Li, S., and Dong, Y. X.: Status, causes and combating suggestions of sandy
653 desertification in Qinghai-Tibet Plateau, Chinese Geogr. Sci., 15, 289-296, doi: 10.1007/s11769-
654 005-0015-9, 2005.
655 Liu, Y. W., Xu-Ri, Xu, X. L., Wei, D., Wang, Y. H., and Wang, Y. S.: Plant and soil responses of an
656 alpine steppe on the Tibetan Plateau to multi-level nitrogen addition, Plant Soil, 373, 515-529,
657 doi: 10.1007/s11104-013-1814-x, 2013.
658 Lu, C. Q., and Tian, H. Q.: Spatial and temporal patterns of nitrogen deposition in China: Synthesis of
659 observational data, J. Geophys. Res.-Atmos., 112, D22S05, doi:10.1029/2006JD007990, 2007.

660 Lu, C. Q., and Tian, H. Q.: Net greenhouse gas balance in response to nitrogen enrichment:
661 perspectives from a coupled biogeochemical model, Glob. Change Biol., 19, 571-588, doi:
662 10.1111/gcb.12049, 2013.
663 Lu, C. Q., and Tian, H. Q.: Half-century nitrogen deposition increase across China: A gridded time-
664 series data set for regional environmental assessments, Atmos. Environ., 97, 68-74, doi:
665 10.1016/j.atmosenv.2014.07.061, 2014.
666 Lu, C. Q., and Tian, H. Q.: Reply to "Comments on 'Half-century nitrogen deposition increase across
667 China: A gridded time-series dataset for regional environmental assessments'", Atmos. Environ.,
668 101, 352-353, doi:10.1016/j.atmosenv.2014.11.032, 2015.
669 Lu, X. W., Li, L. Y., Li, N., Yang, G., Luo, D. C., and Chen, J. H.: Chemical characteristics of spring
670 rainwater of Xi'an city, NW China, Atmos. Environ., 45, 5058-5063, doi:
671 10.1016/j.atmosenv.2011.06.026, 2011.
672 Ma, Y. M., Kang, S. C., Zhu, L. P., Xu, B. Q., Tian, L. D., and Yao, T. D.: Tibetan Observation and
673 Research Platform–atmosphere–land interaction over a heterogeneous landscape, B. Am.
674 Meteorol. Soc., 89, 1487-1492, doi: 10.1175/2008bams2545.1, 2008.
675 Ma, Z., Ma, M. J., Baskin, J. M., Baskin, C. C., Li, J. Y., and Du, G. Z.: Responses of alpine meadow
676 seed bank and vegetation to nine consecutive years of soil fertilization, Ecol. Eng., 70, 92-101,
677 doi: 10.1016/j.ecoleng.2014.04.009, 2014.
678 Mao, R., Gong, D. Y., Shao, Y. P., Wu, G. J., and Bao, J. D.: Numerical analysis for contribution of the
679 Tibetan Plateau to dust aerosols in the atmosphere over the East Asia, Sci. China Earth Sci., 56,
680 301-310, doi: 10.1007/s11430-012-4460-x, 2013.
681 Migliavacca, D., Teixeira, E. C., Wiegand, F., Machado, A. C. M., and Sanchez, J.: Atmospheric
682 precipitation and chemical composition of an urban site, Guaiba hydrographic basin, Brazil,

683 Atmos. Environ., 39, 1829-1844, doi: 10.1016/j.atmosenv.2004.12.005, 2005.
684 Morino, Y., Ohara, T., Kurokawa, J., Kuribayashi, M., Uno, I., and Hara, H.: Temporal variations of
685 nitrogen wet deposition across Japan from 1989 to 2008, J. Geophys. Res.-Atmos., 116, D06307,
686 doi: 10.1029/2010jd015205, 2011.
687 Okay, C., Akkoyunlu, B. O., and Tayanc, M.: Composition of wet deposition in Kaynarca, Turkey,
688 Environ. Pollut., 118, 401-410, doi: 10.1016/S0269-7491(01)00292-5, 2002.
689 Pan, Y. P., Wang, Y. S., Tang, G. Q., and Wu, D.: Wet and dry deposition of atmospheric nitrogen at
690 ten sites in Northern China, Atmos. Chem. Phys., 12, 6515-6535, doi: 10.5194/acp-12-6515-2012,
691 2012.
692 Pinder, R. W., Davidson, E. A., Goodale, C. L., Greaver, T. L., Herrick, J. D., and Liu, L. L.: Climate
693 change impacts of US reactive nitrogen, P. Natl. Acad. Sci. USA, 109, 7671-7675, doi:
694 10.1073/pnas.1114243109, 2012.
695 R Core Team. R: A language and environment for statistical computing. R Foundation for Statistical
696 Computing, Vienna, Austria, 2015.
697 Puxbaum, H., Simeonov, V., Kalina, M., Tsakovski, S., Loffler, H., Heimburger, G., Biebl, P., Weber,
698 A., and Damm, A.: Long-term assessment of the wet precipitation chemistry in Austria (1984-
699 1999), Chemosphere, 48, 733-747, doi: 10.1016/S0045-6535(02)00125-X, 2002.
700 Qiu, J.: The third pole, Nature, 454, 393-396, doi: 10.1038/454393a, 2008.
701 Rodhe, H., and Granat, L.: An evaluation of sulfate in European precipitation 1955-1982, Atmos.
702 Environ., 18, 2627-2639, doi: 10.1016/0004-6981(84)90327-5, 1984.
703 Safai, P. D., Rao, P. S. P., Mornin, G. A., All, K., Chate, D. M., and Praveen, P. S.: Chemical
704 composition of precipitation during 1984-2002 at Pune, India, Atmos. Environ., 38, 1705-1714,
705 doi: 10.1016/j.atmosenv.2003.12.016, 2004.

706 Sahai, S., Sharma, C., Singh, S. K., and Gupta, P. K.: Assessment of trace gases, carbon and nitrogen
707 emissions from field burning of agricultural residues in India, Nutr. Cycl. Agroecosys., 89, 143-
708 157, doi: 10.1007/s10705-010-9384-2, 2011.
709 Shen, W. J., Ren, H. L., Jenerette, G. D., Hui, D. F., and Ren, H.: Atmospheric deposition and canopy
710 exchange of anions and cations in two plantation forests under acid rain influence, Atmos.
711 Environ., 64, 242-250, doi: 10.1016/j.atmosenv.2012.10.015, 2013.
712 Sheng, W. P., Yu, G. R., Jiang, C. M., Yan, J. H., Liu, Y. F., Wang, S. L., Wang, B., Zhang, J. H., Wang,
713 C. K., Zhou, M., and Jia, B. R.: Monitoring nitrogen deposition in typical forest ecosystems along
714 a large transect in China, Environ. Monit. Assess., 185, 833-844, doi: 10.1007/s10661-012-2594-
715 0, 2013.
716 Shi, Y. L., Cui, S. H., Ju, X. T., Cai, Z. C., and Zhu, Y. G.: Impacts of reactive nitrogen on climate
717 change in China, Sci. Rep.-UK, 5, 8118, doi: 10.1038/Srep08118, 2015.
718 Tang, J., Xue, H., Yu, X., Cheng, H., Xu, X., Zhang, X., and Ji, J.: The preliminary study on chemical
719 characteristics of precipitation at Mt. Waliguan, Acta Scientiae Circumstantiae, 20, 420-425, 2000
720 (in Chinese with English abstract).
721 Taylor, S. R.: Abundance of chemical elements in the continental crust - a new table, Geochim.
722 Cosmochim. Ac., 28, 1273-1285, doi: 10.1016/0016-7037(64)90129-2, 1964.
723 Thompson, L. G., Yao, T., Mosley-Thompson, E., Davis, M. E., Henderson, K. A., and Lin, P. N.: A
724 high-resolution millennial record of the South Asian Monsoon from Himalayan ice cores, Science,
725 289, 1916-1919, doi: 10.1126/science.289.5486.1916, 2000.
726 Tripathee, L., Kang, S. C., Huang, J., Sillanpaa, M., Sharma, C. M., Luthi, Z. L., Guo, J. M., and
727 Paudyal, R.: Ionic composition of wet precipitation over the southern slope of central Himalayas,
728 Nepal, Environ. Sci. Pollut. R., 21, 2677-2687, doi: 10.1007/s11356-013-2197-5, 2014.

729 Tu, J., Wang, H. S., Zhang, Z. F., Jin, X., and Li, W. Q.: Trends in chemical composition of precipitation
730 in Nanjing, China, during 1992-2003, Atmos. Res., 73, 283-298, doi:
731 10.1016/j.atmosres.2004.11.002, 2005.
732 Turekian, K. K.: Oceans, Prentice-Hall, New Jersey, United States, 1968.
733 Wang, L. X., and Macko, S. A.: Constrained preferences in nitrogen uptake across plant species and
734 environments, Plant Cell Environ., 34, 525-534, doi: 10.1111/j.1365-3040.2010.02260.x, 2011.
735 Wang, P. L., Yao, T. D., Tian, L. D., Wu, G. J., Li, Z., and Yang, W.: Recent high-resolution
736 glaciochemical record from a Dasuopu firn core of middle Himalayas, Chinese Sci. Bull., 53,
737 418-425, doi: 10.1007/s11434-008-0098-7, 2008.
738 Wang, Y., Ma, Y., Zhu, Z., and Li, M.: Variation characteristics of meteorological elements in near
739 surface layer over the Lulang valley of southeastern Tibetan Plateau, Plateau Meteorology, 29,
740 63-69, 2010 (in Chinese with English abstract).
741 Wang, Y. Q., Zhang, X. Y., and Draxler, R. R.: TrajStat: GIS-based software that uses various trajectory
742 statistical analysis methods to identify potential sources from long-term air pollution
743 measurement data, Environ. Model. Soft., 24, 938-939, doi: 10.1016/j.envsoft.2009.01.004, 2009.
744 Xia, X. G., Wang, P. C., Wang, Y. S., Li, Z. Q., Xin, J. Y., Liu, J., and Chen, H. B.: Aerosol optical
745 depth over the Tibetan Plateau and its relation to aerosols over the Taklimakan Desert, Geophys
746 Res Lett, 35, L16804, doi: 10.1029/2008gl034981, 2008.
747 Xiao, H. W., Xiao, H. Y., Long, A. M., Wang, Y. L., and Liu, C. Q.: Chemical composition and source
748 apportionment of rainwater at Guiyang, SW China, J. Atmos. Chem., 70, 269-281, doi:
749 10.1007/s10874-013-9268-3, 2013.
750 Xu, H., Bi, X. H., Feng, Y. C., Lin, F. M., Jiao, L., Hong, S. M., Liu, W. G., and Zhang, X. Y.: Chemical
751 composition of precipitation and its sources in Hangzhou, China, Environ. Monit. Assess., 183,

581-592, doi: 10.1007/s10661-011-1963-4, 2011.

Xu-Ri, Prentice, I. C., Spahni, R., and Niu, H. S.: Modelling terrestrial nitrous oxide emissions and implications for climate feedback, New. Phytol., 196, 472-488, doi: 10.1111/j.1469-8137.2012.04269.x, 2012.

Xu, X. L., Wanek, W., Zhou, C. P., Richter, A., Song, M. H., Cao, G. M., Ouyang, H., and Kuzyakov, Y.: Nutrient limitation of alpine plants: Implications from leaf N : P stoichiometry and leaf $\delta^{15}N$, J. Plant Nutr. Soil Sc., 177, 378-387, doi: 10.1002/jpln.201200061, 2014.

Yang, F., Tan, J., Shi, Z. B., Cai, Y., He, K., Ma, Y., Duan, F., Okuda, T., Tanaka, S., and Chen, G.: Five-year record of atmospheric precipitation chemistry in urban Beijing, China, Atmos. Chem. Phys., 12, 2025-2035, doi: 10.5194/acp-12-2025-2012, 2012.

Yang, L., Ren, Y., and Jia, L.: Preliminary study of chemical composition of precipitation at Wudaoliang, Qinghai Province, Plateau Meteorology, 10, 209-216, 1991 (in Chinese with English abstract).

Yang, Y. H., Ji, C. J., Ma, W. H., Wang, S. F., Wang, S. P., Han, W. X., Mohammat, A., Robinson, D., and Smith, P.: Significant soil acidification across northern China's grasslands during 1980s-2000s, Glob. Change Biol., 18, 2292-2300, doi: 10.1111/j.1365-2486.2012.02694.x, 2012.

Yang, Z., Ou Yang, H., Xu, X., and Yang, W.: Spatial heterogeneity of soil moisture and vegetation coverage of alpine grassland in permafrost area of the Qinghai-Tibet Plateau, Journal of Natural Resources, 25, 426-434, doi: 10.11849/zrzyxb.2010.03.008, 2010 (in Chinese with English abstract).

Yao, T. D., Masson-Delmotte, V., Gao, J., Yu, W. S., Yang, X. X., Risi, C., Sturm, C., Werner, M., Zhao, H. B., He, Y., Ren, W., Tian, L. D., Shi, C. M., and Hou, S. G.: A review of climatic controls on $\delta^{18}O$ in precipitation over the Tibetan Plateau: observations and simulations, Rev. Geophys., 51,

525–548, doi: 10.1002/rog.20023, 2013.

Yao, T., Thompson, L. G., Mosbrugger, V., Zhang, F., Ma, Y., Luo, T., Xu, B., Yang, X., Joswiak, D. R., Wang, W., Joswiak, M. E., Devkota, L. P., Tayal, S., Jilani, R., and Fayziev, R.: Third Pole Environment (TPE), 3, 52-64, doi:10.1016/j.envdev.2012.04.002, 2012.

Zaehle, S., Friedlingstein, P., and Friend, A. D.: Terrestrial nitrogen feedbacks may accelerate future climate change, Geophys. Res. Lett., 37, 20130125, doi: 10.1029/2009gl041345, 2010.

Zaehle, S., and Friend, A. D.: Carbon and nitrogen cycle dynamics in the O-CN land surface model: 1. Model description, site-scale evaluation, and sensitivity to parameter estimates, Global Biogeochem. Cycles, 24, GB1005, doi: 10.1029/2009gb003521, 2010.

Zaehle, S.: Terrestrial nitrogen - carbon cycle interactions at the global scale, Philos. T. R. Soc. B, 368, L01401, doi: 10.1098/rstb.2013.0125, 2013.

Zbieranowski, A. L., and Aherne, J.: Long-term trends in atmospheric reactive nitrogen across Canada: 1988-2007, Atmos. Environ., 45, 5853-5862, doi: 10.1016/j.atmosenv.2011.06.080, 2011.

Zhang, D. D., Peart, M., Jim, C. Y., He, Y. Q., Li, B. S., and Chen, J. A.: Precipitation chemistry of Lhasa and other remote towns, Tibet, Atmos. Environ., 37, 231-240, doi:10.1016/S1352-2310(02)00835-X, 2003.

Zhang, M., Wang, S., Wu, F., Yuan, X., and Zhang, Y.: Chemical compositions of wet precipitation and anthropogenic influences at a developing urban site in southeastern China, Atmos. Res., 84, 311-322, doi: 10.1016/j.atmosres.2006.09.003, 2007.

Zhang, N. N., He, Y. Q., Cao, J. J., Ho, K. F., and Shen, Z. X.: Long-term trends in chemical composition of precipitation at Lijiang, southeast Tibetan Plateau, southwestern China, Atmos. Res., 106, 50-60, doi: 10.1016/j.atmosres.2011.11.006, 2012.

Zhang, X. Y., Arimoto, R., Cao, J. J., An, Z. S., and Wang, D.: Atmospheric dust aerosol over the

798 Tibetan Plateau, J. Geophys. Res.-Atmos., 106, 18471-18476, doi: 10.1029/2000jd900672, 2001.
799 Zhang, X. Y., Jiang, H., Zhang, Q. X., and Zhang, X.: Chemical characteristics of rainwater in northeast
800 China, a case study of Dalian, Atmos. Res., 116, 151-159, doi: 10.1016/j.atmosres.2012.03.014,
801 2012.
802 Zhang, Y. J., Kang, S. C., You, Q. L., and Xu, Y. W.: Climate in the Nam Co basin, in: Modern
803 environmental processes and changes in the Nam Co basin, Tibetan Plateau, edited by: Kang, S.
804 C., Yang, Y. P., Zhu, L. P., and Ma, Y. M., China Meteorological Press, Beijing, 15-24, 2011 (in
805 Chinese).
806 Zhang, Y. L., Li, B. Y., and Zheng, D.: A discussion on the boundary and area of the Tibetan Plateau
807 in China, Geographical Research, 21, 1-8, 2002 (in Chinese with English abstract).
808 Zhao, H. B., Xu, B. Q., Yao, T. D., Tian, L. D., and Li, Z.: Records of sulfate and nitrate in an ice core
809 from Mount Muztagata, central Asia, J. Geophys. Res.-Atmos., 116, D13304, doi:
810 10.1029/2011jd015735, 2011.
811 Zhao, Z. Z., Cao, J. J., Shen, Z. X., Xu, B. Q., Zhu, C. S., Chen, L. W. A., Su, X. L., Liu, S. X., Han,
812 Y. M., Wang, G. H., and Ho, K. F.: Aerosol particles at a high-altitude site on the Southeast Tibetan
813 Plateau, China: Implications for pollution transport from South Asia, J. Geophys. Res-Atmos.,
814 118, 11360-11375, doi: 10.1002/jgrd.50599, 2013.
815 Zheng, W., Yao, T. D., Joswiak, D. R., Xu, B. Q., Wang, N. L., and Zhao, H. B.: Major ions composition
816 records from a shallow ice core on Mt. Tanggula in the central Qinghai-Tibetan Plateau, Atmos.
817 Res., 97, 70-79, doi: 10.1016/j.atmosres.2010.03.008, 2010.

818 **Table 1. Descriptions of the five precipitation sampling sites on the TP.**

Station name	Station name expanded	Latitude	Longitude	Altitude m a.s.l.	Annual mean temperature ℃	Annual precipitation mm yr^{-1}	Vegetation type	References
Southeast Tibet Station	Southeast Tibet Observation and Research Station for the Alpine Environment, Chinese Academy of Sciences	29°46′N	94°44′E	3326	5.6	800–1000	Subalpine coniferous forest and temperate deciduous conifer mixed forest	Wang et al., (2010)
Nam Co Station	Nam Co Monitoring and Research Station for Multisphere Interactions, Chinese Academy of Sciences	30°47′N	90°58′E	4730	–0.6	414.6	Alpine meadow and alpine steppe	Zhang et al., (2011)
Qomolangma Station	Qomolangma Atmospheric and Environmental Observation and Research Station, Chinese Academy of Sciences	28°13′N	86°34′E	4300	3.9	402.8	Alpine meadow and alpine steppe	Gao et al., (2014) and M. Li et al., (2007)
Ngari Station	Ngari Desert Observation and Research Station	33°24′N	79°43′E	4264	-	124.6	Desert steppe	This study
Muztagh Ata Station	Muztagh Ata Westerly Observation and Research Station	38°17′N	75°1′E	3650	-	213.6	Alpine steppe	This study

819
820
821

822 **Table 2. Annual mean concentrations of major ions (μeq L^{-1}) in precipitation at five remote sites on the TP and other sites in China.** Units of

823 precipitation are millimeters (mm yr^{-1}). VWM indicates volume-weighted mean.

Area	Sites	Represents	Periods	Precipitation	NH_4^+	Na^+	K^+	Mg^{2+}	Ca^{2+}	NO_3^-	Cl^-	SO_4^{2-}	Data type	Reference
Tibetan	Southeast Tibet	Remote site	2011–2012	914.6	4.9	3.8	1.0	0.9	20.8	2.2	2.5	2.1	VWM	This study
Plateau	Nam Co	Remote site	2011–2012	382.5	12.7	1.9	0.4	0.9	7.9	4.5	1.1	2.9	VWM	This study
	Qomolangma	Remote site	2011–2012	258	25.4	26.0	4.5	1.7	53.4	0.8	27.1	3.2	VWM	This study
	Ngari	Remote site	2013	124.6	20.5	12.4	1.8	4.8	50.9	4.8	11.9	11.6	VWM	This study
	Muztagh Ata	Remote site	2011	213.6	42.0	10.1	3.0	11.3	119.4	9.9	8.9	17.4	VWM	This study
	Waliguan	Remote site	1997	388	45.5	8.7	3.8	12.1	34.0	8.3	6.1	24.0	Mean	Tang et al. (2000)
	Wudaoliang	Remote site	Aug. 1989	266.5[a]	27.1	21.7	6.2			13.2	25.6	29.2	Mean	Yang et al. (1991)
	Lhasa	Remote city	1998–2000	250-500	14.3	11.2	5.1	10.9	197.4	6.9	9.7	5.2	Mean	Zhang et al. (2003)
	Lijiang	City	1989–2006	900	11.4	2.5		7.7	50.2	3.6	11.6	32.6	Mean	Zhang et al. (2012a)
				Average	**22.6**	**10.9**	**3.2**	**6.3**	**66.8**	**6.0**	**11.6**	**14.3**		
Northern	Beijing	City	2001–2005	441	236.0	22.5	13.8	48.4	209.0	106.0	34.9	314.0	VWM	F. Yang et al. (2012)
China	Dalian	City	2007	602	107.8	36.2	6.87	25.29	78.92	51.38	59.83	168.0	VWM	Zhang et al. (2012e)
	Nanjing	City	1992–2003	648-1242	193.2	23.0	12.1	31.7	295.4	39.6	142.6	241.8	VWM	Tu et al. (2005)
	Tianshan Mountain	Remote site	1995–1996			55.7	14.9	15.8	78.0	22.3	40.9	88.1	Mean	Hou (2001)
Southern	Hangzhou	City	2006–2008	1435	79.9	12.2	4.2	7.1	51.9	38.4	13.9	110.0	VWM	Xu et al. (2011)
China	NingBo	City	2010–2011	1374.7	46.2	22.4	7.0	9.3	31.5	38.7	31.0	72.6	VWM	Ding et al. (2012)
	Shanghai	City	2005	825.5	80.7	50.1	14.9	29.6	204.0	49.8	58.3	199.6	VWM	K. Huang et al. (2008)
	Shenzhen	City	1986–2006	1769	35.2	40.3	7.2	9.7	77.7	22.1	37.9	74.3	Mean	Y. L. Huang et al. (2008)
	Guiyang	City	2008–2009	1171	112.8	13.9	9.6	10.5	182.9	7.3	20.7	265.6	VMW	Xiao et al. (2013)

824 [a] Precipitation amount data was obtained from Yang et al. (2010).

Table 3. Annual inorganic nitrogen wet deposition (kg N ha^{-1} yr^{-1}) at five remote sites on the TP, as well as other sites in China. Units of precipitation are millimeters (mm yr^{-1}). DIN means inorganic nitrogen (sum of NH_4^+-N and NO_3^--N). VWM indicates volume-weighted mean.

Area	Sites	Represents	Periods	Precipitation	NH_4^+-N	NO_3^--N	DIN	Data type	Reference
Tibetan Plateau	Southeast	Remote site	2011–2012	914.6	0.63	0.28	0.91	VWM	This study
	Nam Co	Remote site	2011–2012	382.5	0.68	0.24	0.92	VWM	This study
	Qomolangma	Remote site	2011–2012	258	0.92	0.03	0.94	VWM	This study
	Ngari	Remote site	2013	124.6	0.36	0.08	0.44	VWM	This study
	Muztagh Ata	Remote site	2011	213.6	1.25	0.30	1.55	VWM	This study
	Waliguan	Remote site	1997	388	2.47	0.45	2.92	Mean	Tang et al. (2000)
	Wudaoliang	Remote site	Aug. 1989	266.5[a]	1.55	1.11	2.66	Mean	Yang et al. (1991)
	Lhasa	Remote city	1998–2000	250-500	0.54	0.45	0.99	Mean	Zhang et al. (2003)
	Naidong	Remote city	2006–2007	451	0.91	0.82	1.72	VWM	Jia (2008)
	Biru	Remote city	2006–2007	582	1.22	1.86	3.08	VWM	Jia (2008)
	Jiangda	Remote city	2006–2007	547	1.11	0.80	1.91	VWM	Jia (2008)
	Lijiang	Remote city	1989–2006	900	1.43	0.46	1.89	Mean	N. N. Zhang et al. (2012)
				Average	**1.09**	**0.57**	**1.66**		
Northern China	Beijing	City	2001–2005	441	14.57	6.54	21.12	VWM	F. Yang et al. (2012)
	Dalian	City	2007	602	9.08	4.33	13.41	VWM	X. Y. Zhang et al. (2012)
	Nanjing	City	1992–2003	648-1242	25.56	5.23	30.79	VWM	Tu et al. (2005)
	Beijing	City	2008–2010	572			27.9	VWM	Pan et al. (2012)
	Tianjin	City	2008–2010	544			18.1	VWM	Pan et al. (2012)
	Baoding	Industrial	2008–2010	513			23.1	VWM	Pan et al. (2012)
	Tanggu	Industrial	2008–2010	566			28.2	VWM	Pan et al. (2012)
	Tangshan	Industrial	2008–2010	610			21.6	VWM	Pan et al. (2012)
	Yangfang	Suburban	2008–2010	404			20.7	VWM	Pan et al. (2012)
	Cangzhou	Suburban	2008–2010	605			22.6	VWM	Pan et al. (2012)
	Luancheng	Agricultural	2008–2010	517			22.2	VWM	Pan et al. (2012)
	Yucheng	Agricultural	2008–2010	566			24.8	VWM	Pan et al. (2012)
	Xinglong	Rural	2008–2010	512			16.3	VWM	Pan et al. (2012)
Southern China	TieShanPing	Remote site	1999–2004	1228	25.50	9.80	35.30	VWM	Chen and Mulder (2007)
	LiuChongGuan	Remote site	1999–2004	854	2.40	1.30	3.70	VWM	Chen and Mulder (2007)
	LeiGongShan	Remote site	1999–2004	1714	3.70	2.60	6.30	VWM	Chen and Mulder (2007)
	CaiJiaTang	Remote site	1999–2004	1232	21.10	12.70	33.80	VWM	Chen and Mulder (2007)
	LiuXiHe	Remote site	1999–2004	1620	4.30	7.50	11.80	VWM	Chen and Mulder (2007)
	Hangzhou	City	2006–2008	1435	16.1	7.7	23.77	VWM	Xu et al. (2011)
	Ningbo	City	2010–2011	1374.7	8.9	7.4	16.34	VWM	Ding et al. (2012)
	Shanghai	City	2005	825.5	9.3	5.8	15.08	VWM	K. Huang et al. (2008)
	Shenzhen	City	1986–2006	1769	8.7	5.5	14.19	Mean	Y. L. Huang et al. (2008)
	Guiyang	City	2008–2009	1171	18.5	1.2	19.69	VMW	Xiao et al. (2013)

Notes: Tang et al. (2000), Yang et al. (1991), Zhang et al. (2003), N. N. Zhang et al. (2012), F. Yang et al. (2012), X. Y. Zhang et al. (2012), Xu et al. (2011), Ding et al. (2012), K. Huang et al. (2008), Y. L. Huang et al. (2008) and Xiao et al. (2013) reported the concentrations of NH_4^+-N and NO_3^--N in precipitation, but did not calculate nitrogen wet deposition. For these previous studies, we recalculated the annual inorganic nitrogen wet deposition according to the reported

concentrations of NH_4^+-N and NO_3^--N in precipitation and annual precipitation. [a] Precipitation amount data was obtained from Yang et al. (2010).

Table 4. Enrichment factors relative to seawater and soil for precipitation constituents of five remote sites on the TP.

	Southeast Tibet Station		Nam Co Station		Qomolangma Station		Ngari Station		Muztagh Ata Station		$[X/Na^+]_{sea}$	$[X/Ca^{2+}]_{soil}$
	EF_{sea}	EF_{soil}	EF_{sea}	EF_{soil}	EF_{sea}	EF_{soil}	EF_{sea}	EF_{soil}	EF_{sea}	EF_{soil}		
Na^+	1.0	0.36	1.0	0.48	1.0	0.99	1.0	0.5	1.0	0.17	1.0000	0.5690
NH_4^+	15707	350	80684	2378	11629	701	19706	594	49751	519	0.0001[a]	0.0006[c]
K^+	11.5	0.18	8.5	0.17	7.83	0.33	6.4	0.13	13.5	0.10	0.0220	0.5040
Mg^{2+}	1.1	0.05	2.0	0.12	0.29	0.03	1.7	0.10	4.9	0.10	0.2270	0.5610
Ca^{2+}	126.2	1.0	95.3	1.0	46.6	1.0	93.1	1.0	269.5	1.0	0.0440	1.0000
Cl^-	0.57	67.3	0.50	77.8	0.90	286	0.8	132	0.76	42.2	1.1600	0.0031
NO_3^-	23842	154	98242	840	1237	21.7	15869	139	40619	123	0.0000[b]	0.0021[d]
SO_4^{2-}	4.7	13.0	12.7	46.7	1.03	7.76	7.7	29.2	14.3	18.6	0.1210	0.0188[e]

[a] Marine nitrogen ions regarded as entire NH_4^+.

[b] Marine nitrogen ions regarded as entire NO_3^-.

[c] Soil nitrogen regarded as entire range of NH_3 compounds.

[d] Soil nitrogen regarded as entire range of NO_3 compounds.

[e] Soil sulfur regarded as entire range of SO_4 compounds.

842 **Table 5. Source contributions (%) for major ions in precipitation of five remote sites on the TP.**

843 SSF indicates sea salt fraction; CF indicates crust fraction; AF indicates anthropogenic fraction.

	Southeast Tibet Station			Nam Co Station			Qomolangma Station			Ngari Station			Muztagh Ata Station		
	SSF	CF	AF	SSF	CF	AF	SSF	CF	AF	SSF	CF	AF	SSF	CF	AF
NH_4^+	0.0	0.3	**99.7**	0.0	0.0	**100**	0.0	0.1	**99.8**	0.0	0.2	**99.8**	0.0	0.2	**99.8**
NO_3^-	0.0	0.6	**99.3**	0.0	0.1	**99.9**	0.1	4.6	**95.3**	0.0	0.7	**99.3**	0.0	0.8	**99.2**
SO_4^{2-}	21.3	7.7	**71.0**	7.9	2.1	**90.0**	**87.1**	12.9		12.9	3.4	**83.7**	7.0	5.4	**87.6**
Ca^{2+}	0.8	**99.2**		1.0	**99.0**		2.1	**97.9**		1.1	**98.9**		0.4	**99.6**	
K^+	8.7	**91.3**		11.8	**88.2**		12.8	**87.2**		15.5	**84.5**		7.4	**92.6**	
Mg^{2+}	**92.9**	7.1		49.0	**51.0**		0	**100**		**59.2**	40.8		20.2	**79.8**	
Cl^-	**98.5**	1.5		**98.7**	1.3		**99.7**	0.3		**99.2**	0.8		**97.6**	2.4	
Na^+	**100**			**100**			**100**			**100**			**100**		

844

Table 6: Varimax-rotated principal component analysis of major ions in precipitation at five remote sites on the TP. PC1, PC2 and PC3 indicates the 1st, 2nd and 3rd component, respectively. CT means communality. *N* indicates the number of precipitation samples at each site. Boldfaced values are the largest value among the 3 component for each ion.

	Southeast Tibet (*N* = 53)				Nam Co (*N* = 27)				Qomolangma (*N* = 30)				Ngari (*N* = 39)				Muztagh Ata (*N* = 19)			
	RC1	RC2	RC3	CT	RC1	RC2	RC3	CT	RC1	RC2	RC3	CT	RC1	RC2	RC3	CT	RC1	RC2	RC3	CT
Na^+	**0.94**	0.02	0.24	0.94	0.62	**0.73**	0.00	0.93	**0.91**	0.28	0.10	0.92	0.62	**0.73**	0.06	0.92	0.22	**0.96**	0.08	0.98
NH_4^+	0.25	0.22	**0.93**	0.98	0.36	0.13	**0.89**	0.94	**0.69**	-0.15	0.24	0.56	-0.11	0.57	**0.75**	0.90	-0.19	0.14	**0.96**	0.98
K^+	**0.88**	0.10	0.35	0.91	0.11	**0.93**	0.07	0.89	**0.84**	0.35	0.27	0.89	0.15	**0.84**	0.40	0.89	0.47	**0.79**	-0.05	0.85
Mg^{2+}	**0.77**	0.45	0.29	0.89	**0.89**	0.19	0.38	0.97	0.39	**0.88**	0.18	0.97	**0.67**	0.56	0.09	0.78	**0.90**	0.38	-0.16	0.99
Ca^{2+}	**0.66**	0.46	0.21	0.70	**0.76**	0.11	0.57	0.92	-0.02	**0.96**	0.03	0.92	**0.85**	0.17	0.15	0.77	**0.85**	0.35	-0.25	0.90
Cl^-	**0.91**	0.10	-0.06	0.85	0.05	**0.95**	0.20	0.95	**0.92**	0.25	0.11	0.92	0.37	**0.83**	0.00	0.82	0.25	**0.92**	0.17	0.94
NO_3^-	0.03	**0.95**	0.09	0.91	0.32	0.13	**0.92**	0.96	0.26	0.16	**0.94**	0.98	0.36	-0.01	**0.84**	0.84	**0.88**	0.12	-0.18	0.83
SO_4^{2-}	0.24	**0.89**	0.18	0.89	**0.80**	0.10	0.52	0.92	**0.64**	**0.64**	0.31	0.90	**0.91**	0.22	0.15	0.90	**0.87**	0.31	0.11	0.87
Variance (%)	46	27	15		33	30	30		43	30	15		34	33	19		43	35	14	
Cumulative (%)	46	73	88		33	63	93		43	74	88		34	66	85		43	78	92	

Figure captions

Figure 1. Map of the precipitation nitrogen wet deposition sampling sites on the TP. The red points indicate the five remote sampling stations of this study. The black points indicate the sampling sites from previous records. Southeast Tibet Station is short for Southeast Tibet Observation and Research Station for the Alpine Environment, Chinese Academy of Sciences; Nam Co Station is short for Nam Co Monitoring and Research Station for Multisphere Interactions, Chinese Academy of Sciences; Qomolangma Station is short for Qomolangma Atmospheric and Environmental Observation and Research Station, Chinese Academy of Sciences; Ngari Station is short for Ngari Desert Observation and Research Station; and Muztagh Ata Station is short for Muztagh Ata Westerly Observation and Research Station.

Figure 2. Seasonal dynamics of ion concentrations (unit: μeq L^{-1}) and precipitation (unit: mm) at five remote sites on the TP. The sampling times of the five stations were as follows: Southeast Tibet Station, November 2011 to October 2012; Nam Co Station, August 2011 to July 2012; Qomolangma Station, April 2011 to March 2012; Ngari Station, January 2013 to December 2013; Muztagh Ata Station, January 2011 to December 2011.

Figure 3. Annual average volume-weighted concentration percentages of measured ions in precipitation (unit: μeq L^{-1}/μeq L^{-1}) at five remote sites on the TP.

Figure 4. Seasonal dynamics of inorganic N wet deposition at five remote sites on the TP. The sampling time windows of those stations are same to Fig. 2.

Figure 5. Seven-day backward trajectories at five remote sites on the TP. Black lines show the backward trajectories calculated at 6-h interval (00:00, 06:00, 12:00, 18:00 UTC) at sampling days, with an arrival height of 500 m above the ground. Red lines show the clustering trajectories.

872 **Figure 1.**

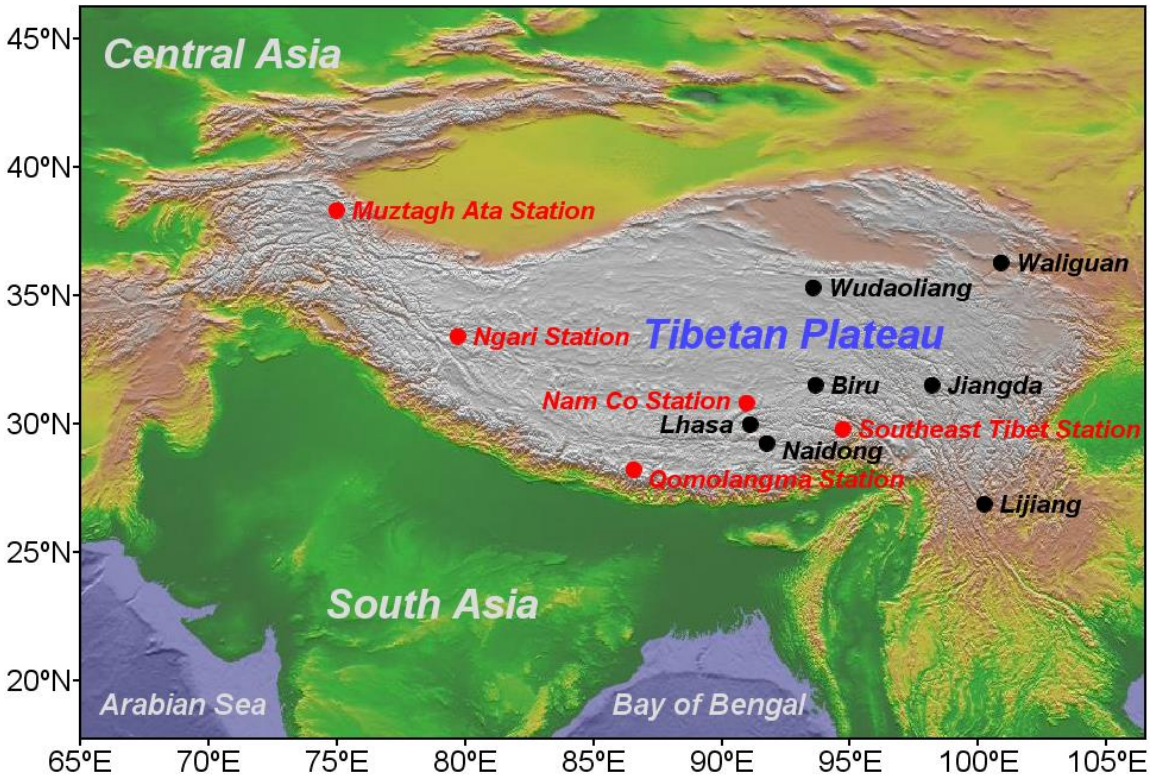

873

874 **Figure 2.**

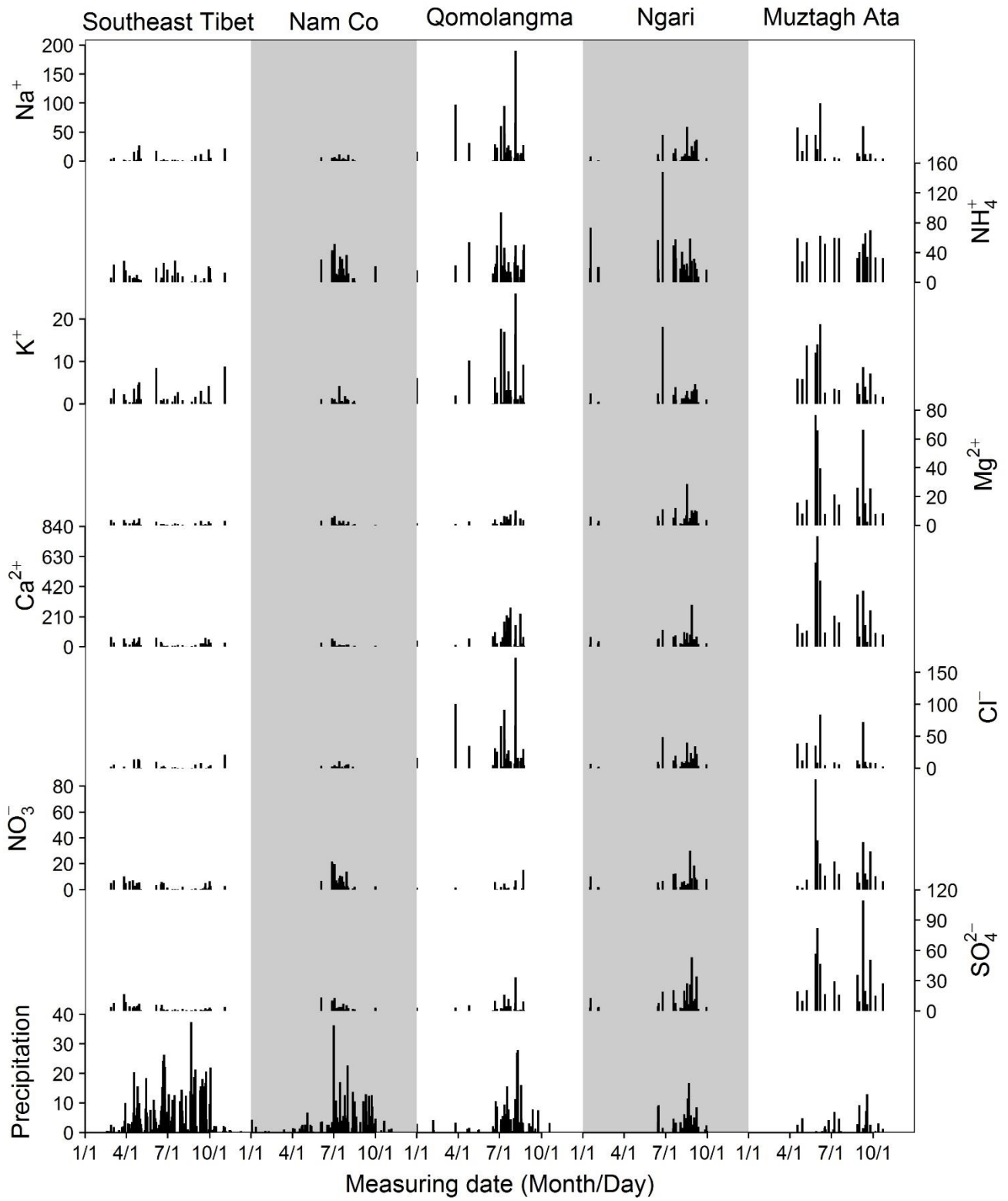

875

876 **Figure 3.**

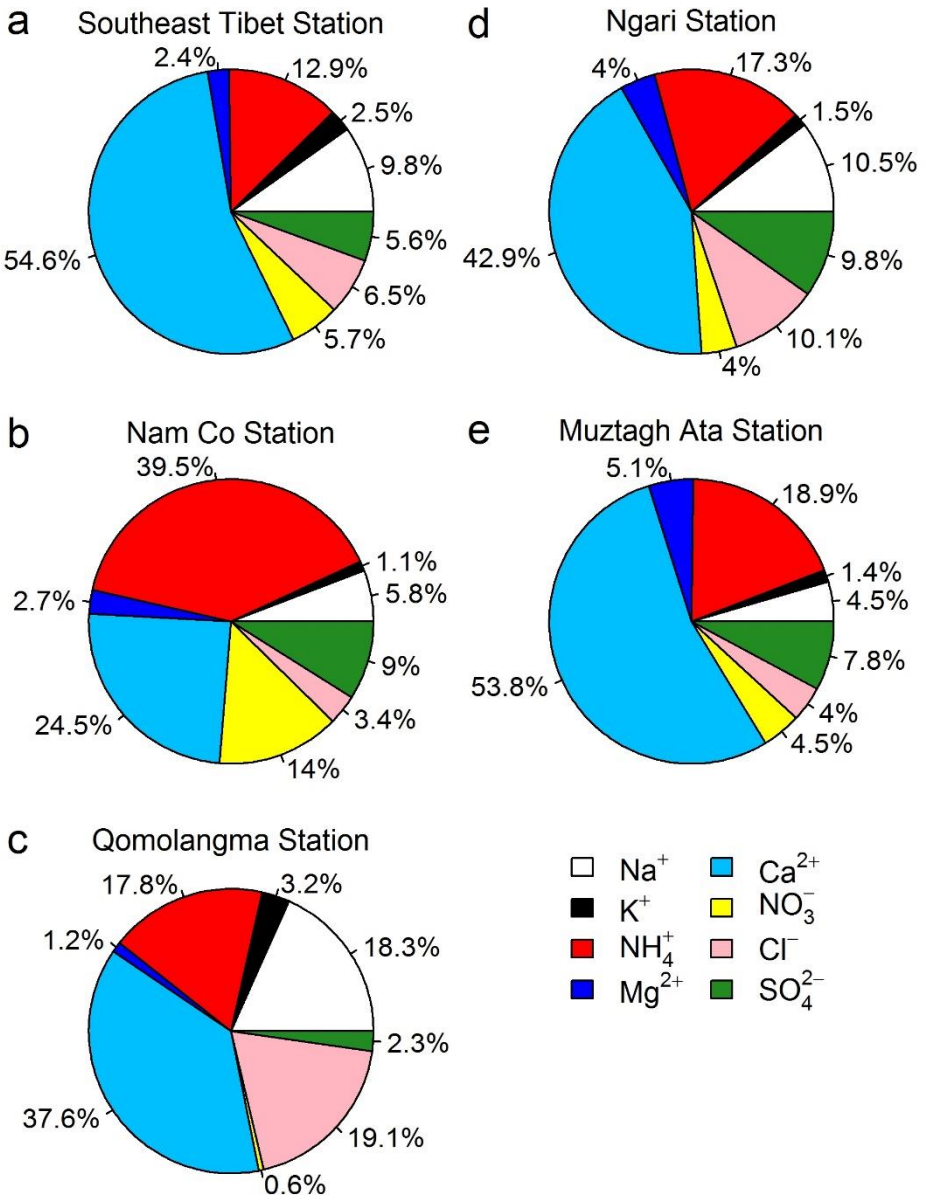

877

878

879 **Figure 4.**

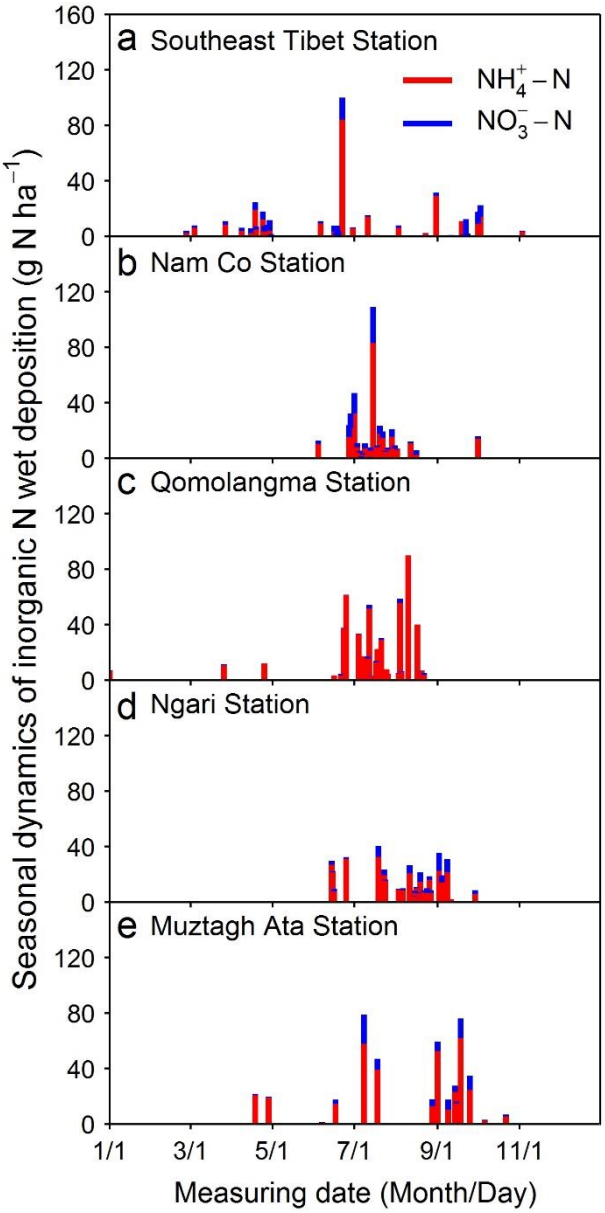

880
881

882 **Figure 5.**

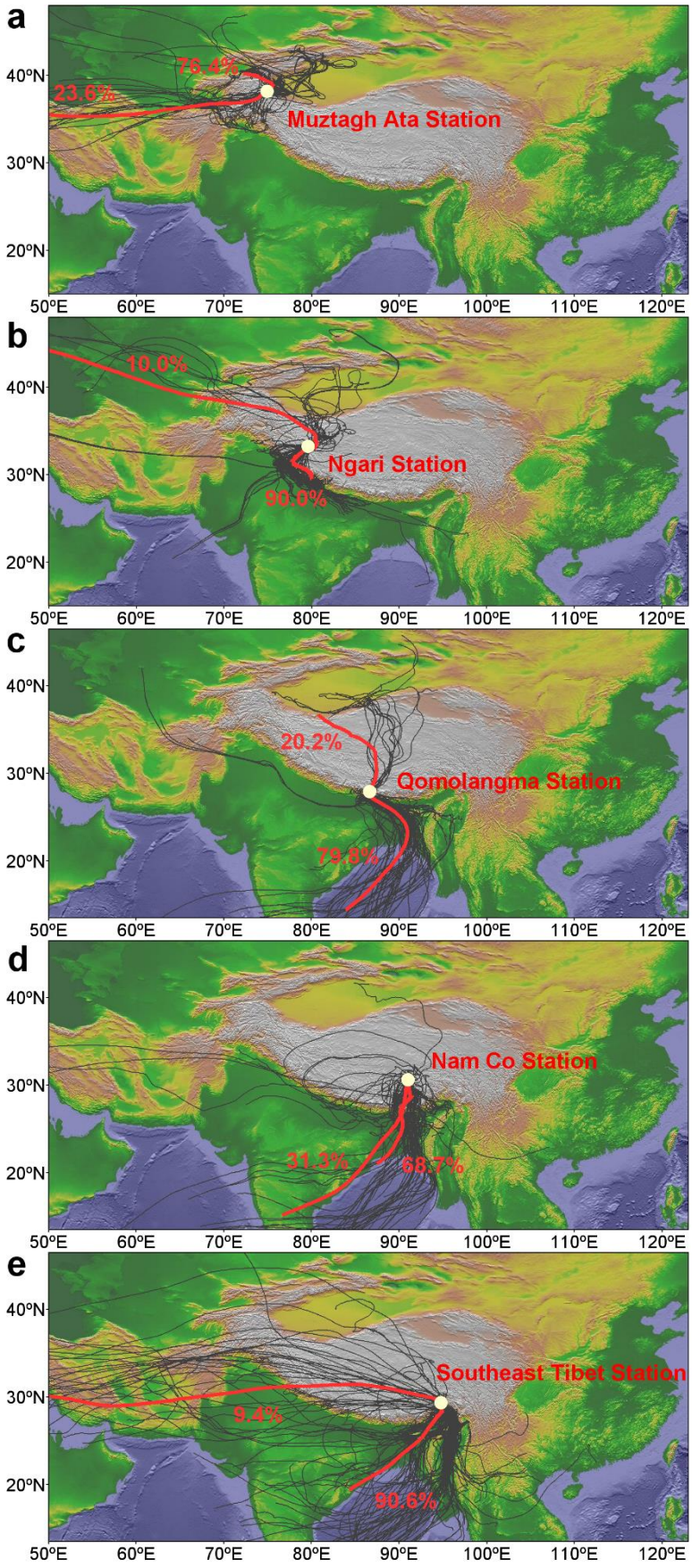

883